Studying connectivity in the neonatal EEG

Anton Tokariev

Neuroscience Center and
Division of Physiology and Neuroscience
Department of Biosciences
Faculty of Biological and Environmental Sciences
University of Helsinki

Doctoral Program in Brain & Mind

ACADEMIC DISSERTATION

To be presented for public examination with the permission of the
Faculty of Biological and Environmental Sciences of the
University of Helsinki
In the lecture hall 2402, Viikki Biocenter 3 (Viikinkaari 1, Helsinki)
On August 18th at 12 noon.

Helsinki 2015

Supervised by

Docent **Sampsa Vanhatalo**, MD, PhD
Department of Clinical Neurophysiology,
HUS Medical Imaging Center,
Helsinki University Central Hospital and
University of Helsinki, Finland

Docent **J. Matias Palva**, PhD
Neuroscience Center, University of Helsinki, Finland

Thesis advisory committee

Professor **Ari Koskelainen**, PhD
Department of Biomedical Engineering and Computational Science
Aalto University, Finland

PhD **Alexander Zhigalov**
Neuroscience Center, University of Helsinki, Finland

Pre-examiners

Professor **Ingmar Rosén**, MD, PhD
Department of Clinical Sciences,
Lund University, Sweden

Assistant Professor **Lauri Parkkonen**, PhD
Department of Biomedical Engineering and Computational Science
Aalto University, Finland

Opponent

Docent **Ari Pääkkönen**, PhD
Diagnostic Imaging Centre,
Kuopio University Hospital, Finland

Custos

Professor **Juha Voipio**, PhD
Department of Biosciences
University of Helsinki, Finland

Dissertationes Scholae Doctoralis Ad Sanitatem Investigandam Universitatis Helsinkiensis

ISBN 978-951-51-1409-9 (paperback)
ISBN 978-951-51-1410-5 (PDF, http://ethesis.helsinki.fi)
ISSN 2342-3161 (Print)
ISSN 2342-317X (Online)

Hansaprint, Vantaa 2015

To my Family

CONTENTS

LIST OF ORIGINAL PUBLICATIONS

This Thesis is based on the following publications which are referred to in Roman numerals in the text:

I. **Tokariev, A.**, Palmu, K., Lano, A., Metsäranta, M., Vanhatalo, S., 2012. Phase synchrony in the early preterm EEG: development of methods for estimating synchrony in both oscillations and events. Neuroimage. 60, 1562–1573.

II. Odabaee, M., **Tokariev, A.**, Layeghy, S., Mesbah, M., Colditz, P.B., Ramon, C., Vanhatalo, S., 2014. Neonatal EEG at scalp is focal and implies high skull conductivity in realistic neonatal head models. Neuroimage. 96, 73–80.

III. **Tokariev, A.**, Vanhatalo, S., Palva J.M., 2015. Analysis of infant cortical synchrony is constrained by the number of recording electrodes and the recording montage. Clin Neurophysiol. doi:10.1016/j.clinph.2015.04.291

Author's contribution to the studies included to the Thesis:

Study I: The author developed the algorithm for analyzing synchronization in events and oscillations in the preterm EEG, performed data analysis, and wrote the manuscript together with SV.

Study II: The author performed MRI data pre-processing, generated the boundary element method (BEM) neonatal head model, carried out all computational simulations with BEM model, and wrote the corresponding sections for the paper.

Study III: The author participated in the design of the experiments, generated BEM head model and performed computer simulations, analyzed the data and wrote the manuscript together with SV and MP.

Publications that have been used in other dissertations:

Study II will be used in the dissertation work by Maryam Odabaee (University of Queensland, Brisbane, Queensland, Australia). Title: 'Neonatal EEG source localization using enhanced time-frequency multiple signal classification' (to be submitted in 2015).

List of abbreviations

3D	Three dimensional
AP	Action potential
AS	Active sleep
BAF	Band amplitude fluctuation
BEM	Boundary elements method
CA	Conceptional age
cPLV	Complex phase locking value
CSD	Current source density
CSF	Cerebro-spinal fluid
DC	Direct current
EEG	Electroencephalography
EPSP	Excitatory postsynaptic potential
ERP	Evoked response potential
FEM	Finite element method
FFT	Fast Fourier Transform
FIR	Finite impulse response
GA	Gestational age
GABA	γ-aminobutyric acid
hdEEG	High-density electroencephalography
IIR	Infinite impulse response
iPLV	Imaginary part of the phase locking value
IPSP	Inhibitory postsynaptic potential
inter-SAT	Interval between the spontaneous activity transients
IVH	Intraventricular hemorrhage
MRI	Magnetic resonance imaging
NICU	Neonatal intensive care unit
P.V.	Principal Value
PLV	Phase locking value
PS	Phase synchrony
QS	Quiet sleep
RMS	Root mean square
rPLV	Real part of the phase locking value
SAT	Spontaneous activity transient
SD	Standard deviation

ABSTRACT

In humans the few months surrounding birth comprise a developmentally critical period characterised by the growth of major neuronal networks as well as their initial tuning towards more functionally mature large-scale constellations. Proper wiring in the neonatal brain, especially during the last trimester of pregnancy and the first weeks of postnatal life, relies on the brain's endogenous activity and remains critical throughout one's life. Structural or functional abnormalities at the stage of early network formation may result in a neurological disorder later during maturation. Functional connectivity measures based on an infant electroencephalographic (EEG) time series may be used to monitor these processes.

A neonatal EEG is temporally discrete and consists of events (e.g., spontaneous activity transients (SATs)) and the intervals between them (inter-SATs). During early maturation, communication between areas of the brain may be transmitted through two distinct mechanisms: synchronisation between neuronal oscillations and event co-occurrences. In this study, we proposed a novel algorithm capable of assessing the coupling on both of these levels. Our analysis of real data from preterm neonates using the proposed algorithm demonstrated its ability to effectively detect functional connectivity disruptions caused by brain lesions. Our results also suggest that SAT synchronisation represents the dominant means through which inter-areal cooperation occurs in an immature brain. Structural disturbances of the neuronal pathways in the brain carry a frequency selective effect on the functional connectivity decreasing at the event level.

Next, we used mathematical models and computational simulations combined with real EEG data to analyse the propagation of electrical neuronal activity within the neonatal head. Our results show that the conductivity of the neonatal skull is much higher than that found in adults. This leads to greater focal spread of cortical signals towards the scalp and requires high-density electrode meshes for quality monitoring of neonatal brain activity. Additionally, we show that the specific structure of the neonatal skull *fontanel* does not represent a special pathway for the spread of electrical activity because of the overall high conductivity of the skull.

Finally, we demonstrated that the choice of EEG recording montage may strongly affect the fidelity of non-redundant neuronal information registration as well as the output of functional connectivity analysis. Our simulations suggest that high-density EEG electrode arrays combined with mathematical transformations, such as the global average or current source density (CSD), provide more spatially accurate details about the underlying cortical activity and may yield results more robust against volume conduction effects. Furthermore, we provide clear instruction regarding how to optimise recording montages for different numbers of sensors.

1. INTRODUCTION

The final months of pregnancy and the first weeks of life are critical for the development of the human brain. During that time, the major brain networks are physically and functionally established, and the brain functions are exquisitely sensitive to environmental effects. These realities make the neonatal brain unique and call for the particular need to carefully monitor it during the prenatal and postnatal periods. Abnormalities or improper structural connectivity during early maturation may manifest much later in life as cognitive disorders. Thus, the assessment of infant brain activity may assist in the early diagnosis and prediction of neurodevelopmental disorders.

Electroencephalography (EEG) is a widely used, clinically suitable technique to measure infant brain activity. Connectivity analysis applied to multichannel neonatal EEG represents a promising approach to assess the dynamics of neuronal large-scale network formation. Brain areas are established to interact by synchronising their electrical activity (Singer 1999; Fries 2005; Bressler and Menon 2010; Uhlhaas et al. 2010; Palva and Palva 2011). The synchronisation of neuronal activity between neurons and their clusters also plays an important role during development. Hence, connectivity analysis commonly focuses on the synchrony estimation between neuronal oscillations (Palva and Palva 2012; Engel et al. 2013).

Neonatal EEG possesses specific features and is characterised by the presence of temporally discrete spontaneous activity transients (SATs) believed to play a crucial role in guiding and supporting early network organization (Vanhatalo et al. 2005a; Vanhatalo and Kaila 2006; Vanhatalo and Kaila 2010). Different conductivity properties of the tissues and the geometry of the infant head make the spread of electrical cortical activity towards recording EEG sensors quite distinct from adults. Therefore, this should be taken into account when performing connectivity analysis on infant EEG data.

2. REVIEW OF THE LITERATURE

2.1. Changes in the developing brain

Beginning from an early preterm age, dramatic structural and functional changes occur in an infant's brain. During the third trimester (weeks 29 to 40), the human brain nearly triples its size in volume and continues actively growing such that by the age of one year it reaches about 70% of its adult size (Dekaban 1978; Hüppi et al. 1998; Kapellou et al. 2006; Knickmeyer et al. 2008). At the same time, cortical surface folding takes place leading to an overall surface increase and to the formation of the sulci and gyri, changing their configuration with maturation (Kapellou et al. 2006; Dubois et al. 2008b). Some research suggests that during evolution the brain developed its optimal geometry in terms of area allocation and the network organisation between them when space is limited (Chklovskii et al. 2002; Klyachko and Stevens 2003; Cherniak et al. 2004). Thus, structural changes during maturation are aimed at reaching this optimum.

The most critical period for infant brain development is most likely the third trimester. Research on humans and animal models shows that an immature brain is characterised by the presence of a temporary thick neuronal structure called the *'subplate'* underlying the cortical layer (Molliver et al. 1973; Kostovic and Rakic 1990; Kostovic and Judas 2006). At a gestational age (GA) of 18 to 22 weeks, the subplate is about five times thicker than the cortex (Tau and Peterson 2010). Towards full-term, the thickness gradually decreases, disappearing during postnatal development (McConnell et al. 1989). This structure plays an important role during early development and performs the function of a 'waiting' zone, where afferents from the thalamus and other cortical regions establish the first long-range connections (Kostovic and Judas 2006). At the end of the second trimester (around 28 weeks), thalamocortical connections reach the subplate layer, but corticocortical connections have not yet grown. At the beginning of the third trimester (weeks 29 to 33), thalamocortical connections are set in the cortical layer while corticocortical connections attain the subplate and lower cortical structures. Closer to full-term (weeks 38 to 40), thalamocortical connections are established primarily in the cortical layer IV, while corticocortical connections also reach their target zones in the cortex (Kostovic and Jovanov-Milosevic 2006; Vanhatalo and Kaila 2006).

The formation of short-range corticocortical compared to long-range connections is delayed time-wise and strictly related to the differentiation of cortical neurons (Mountcastle 1997; Ramakers 2005; Vanhatalo and Kaila 2006). The six-layer organisation of the cortex and differentiation between its areas are already visible around 31 weeks GA (Mrzljak et al. 1988).

During the third trimester, a peak of axonal myelination also occurs (Dubois et al. 2014). Myelin is a fatty substance produced by glia cells which wraps around axons increasing the efficiency of information transfer between neurons and their networks. This process lasts for a few years after birth and affects various axonal tracts at different times (Yakovlev and Lecours 1967).

All these on-going processes in the neonatal brain have their own, partly overlapping, time spans.

2.2. Structural and functional connectivity

In neuroscience, *structural connectivity* refers to the anatomical links between neurons and their populations (such as synapses or fibres) enabling interactions between them. Structural connectivity features a relatively steady configuration over a time scale ranging from hours up to days. In the developing brain where axonal projections are actively growing and synaptic connections are setting and pruning (synaptogenesis), physical reshaping of the networks is more dynamic and occurs on a larger scale compared to those in adults. In turn, *functional connectivity* refers interaction between brain areas, which is often measures as a synchronisation of neuronal activity from, for instance, pairs of EEG time series. The time scale of single episodes of functional interaction is often brief, in the order of tens of milliseconds (Sporns 2011). Functional connectivity may be assessed from a series of measurements using various techniques including EEG. Both types of connectivity are highly interrelated. Canadian psychologist Donald Hebb (Hebb 1949) formulated a classical rule in neuroscience: 'neurons that fire together wire together'. This also applies to neuronal populations. Thus, estimating functional connectivity may be efficiently used to track structural changes and abnormalities in brain networks, making this approach particularly valuable in the context of monitoring developing brains (Vanhatalo and Palva 2011; Palva and Palva 2012).

In the first place, the neonatal brain sets up most of the structural connections between its neuronal populations. The development of functional connectivity for various neuronal networks may occur at distinct time periods. For example, prominent development of functional connectivity in sensory networks is already seen during the first year of life, whereas visual networks develop during the second year (Lin et al. 2008). Networks related to cognitive functioning develop much later (Doria et al. 2010). Improper structural connections established during prenatal and perinatal periods, however, may lead to neurocognitive disorders later in life (Dudink et al. 2008; Dubois et al. 2008a; Kostovic and Judas 2010).

2.3. Role of neuronal synchrony

The human brain is an extremely complex system with optimal hierarchical organisation constrained by physical limits. Despite the fact that the brain possesses billions of neurons, it is impossible to pinpoint a particular region capable of processing any specific object or disturbance offered by the external world as a whole. Thus, the brain operates based on two main interconnected principles: segregation and integration (Tononi et al. 1994). The first one simply means that separate specialised neurons and their populations in the brain are responsible for specific features of recognition. The latter principle refers to the fact that information from these distinct populations is summated or bound together on higher hierarchical levels. The key mechanism needed to allow for this binding is the simultaneous (synchronous) activation of these segregated areas (Singer 1999; Varela et al. 2001). This principle is fundamental to communication along different scales in the brain: from neurons up to their populations. In neurobiology, it is also called *coincidence detection*, meaning that temporally close appearances of different neuronal inputs from spatially distributed sources make it possible for neurons and their circuits to encode information (Joris et al. 1998; Bender et al. 2006). Previous research also showed in children and adults that most of the higher brain functions (such as perception and cognition) involve multiple areas that interact through their neuronal activity synchronisation (Bressler and Menon 2010; Uhlhaas et al. 2010). In the developing brain, when huge amounts of synaptic connections are forming and pruning, neuronal activity synchronisation manages these processes and, thus, plays an important role for the self-organisation of networks (Singer 1995; Ben-Ari 2001; Khazipov and Luhmann 2006). Therefore, synchronous activity enables information integration and communication, and may influence the shaping of networks in the brain during maturation as well as the functional segregation of neurons (Hanganu-Opatz 2010; Kilb et al. 2011; Omidvarnia et al. 2014b).

In preterm infants, the change in cooperation between brain areas is highly related to the synchronisation of SATs (Vanhatalo et al. 2005a; Vanhatalo and Kaila 2006). Two distinct mechanisms may trigger the interplay between neuronal populations: synchronisation between nested oscillations within SATs and co-occurrence of SAT events. In the neonatal brain at an early preterm age, connections between different cortical areas as well as between the cortex and thalamus are growing. Without existing direct or indirect structural connections, the interplay between distinct brain areas is physically impossible. At that time, SATs in two hemispheres behave more autonomously, with poor synchrony, at times only unilaterally, and their bilateral co-incidence more likely relates to the same underlying triggering mechanism. Thus, synchrony plays a guiding function in the early networking processes in the brain using its own endogenous activity (Katz 1993; Katz and Shatz 1996) and, later, in the maturation of sensory inputs. Towards full-term age,

the coincidence of SATs between the hemispheres becomes more synchronized. This is partly associated with the establishment of callosal connections making communication between hemispheres possible (Vanhatalo and Kaila 2006) and, consequently, enabling the activity-based tuning of interhemispheric cooperation. Beginning during the postnatal period alongside structural wiring, maturation of the inhibitory GABAergic system, and myelination of axonal tracts, synchronisation of neuronal activity configures and sculptures the networks in the brain through early adulthood. For this reason, tracking synchrony starting from an early preterm age is important and may provide information about structural or functional abnormalities during development.

2.4. EEG measurement

Electroencephalography (EEG) is a technique for recording electrical activity in the brain. The history of EEG begins early in 1875 when physician Richard Carton successfully recorded electrical activity from the neocortex of rabbits and monkeys. The next significant date for the technique was 1924 when German psychiatrist Hans Berger successfully recorded the first human EEG using a device called an *electroencephalograph*.

The first EEG data from normal neonates was published in 1938 (Loomis et al. 1938; Smith 1938) and, more than a decade later in 1951, two independent groups simultaneously reported the first EEG data from preterm infants (Hughes et al. 1951; Mai et al. 1951). Today, existing facilities and technologies available in most neonatal intensive care units (NICU) in developed countries allow for the recording of multichannel EEG data starting with early preterm infants (at a GA from about 24 weeks).

In the conventional EEG routine, electrical brain activity is recorded using a set of passive sensors (electrodes) placed on the scalp surface. In most applications, electrodes are placed according to the international 10–20 system (Jasper 1958; Towle et al. 1993), but their number may vary depending on the specific goal of the analysis. For research purposes, up to hundreds of sensors may be used. In most clinical applications, however, using 19 recording electrodes represents the common practice. Traditionally, for neonatal EEG recording, an even lower number of sensors are used (André et al. 2010). Several recent studies demonstrated the advantage of using high-density sensors arrays for EEG recordings from infants both for clinical and research purposes (Grieve et al. 2003; Grieve et al. 2004; Wallois et al. 2009; Odabaee et al. 2013; Omidvarnia et al. 2014b).

Physically, EEG represents the difference in the potential between two spatially distinct points on the scalp. This difference can be taken either between certain pairs of scalp electrodes or between the potential in every electrode relative to some virtual reference point. How EEG signals

are represented is referred to as a *montage*. Bipolar montages show EEG signals derived by subtracting electrical potentials between neighbouring sensors along a defined direction such as *banana* (from front to back) and *transverse* (from left to right). A monopolar montage refers to the difference between all electrodes and that designated as the reference, which as a rule is located at the midline (rendering the reference equidistant from both hemispheres and relatively silent). The *linked mastoids* reference point is derived as an average from two additional electrodes placed on the ears, with the result subtracted from all other recording sensors (see also Figure 1B). Virtual montages relate to the grand *average* reference (difference between each electrode and global mean from all electrodes; Goldman 1950; Offner 1950) and the *Laplacian* transform also called the *current source density* (CSD; difference between electrode and weighted average of its neighbours; Hjorth 1975; Kayser and Tenke 2006a; Kayser and Tenke 2006b; Tenke and Kayser 2012). The latter two montages are also called *mathematical* and may be computed independently of the reference used in the EEG recordings.

A proper or 'optimal' choice for the EEG recording reference point in the literature is usually called the *reference problem*. Others demonstrated that the choice of the reference may affect the output of some EEG analyses (Wolpaw and Wood 1982; Pascual-Marqui and Lehmann 1993; Nunez et al. 1997; Essl and Rappelsberger 1998; Mima and Hallett 1999; Nunez et al. 1999; Hagemann et al. 2001; Yao et al. 2005; Yao et al. 2007). In most studies of this problem, researchers report different analytical results obtained using various references and validate their performance based on *a priori* knowledge.

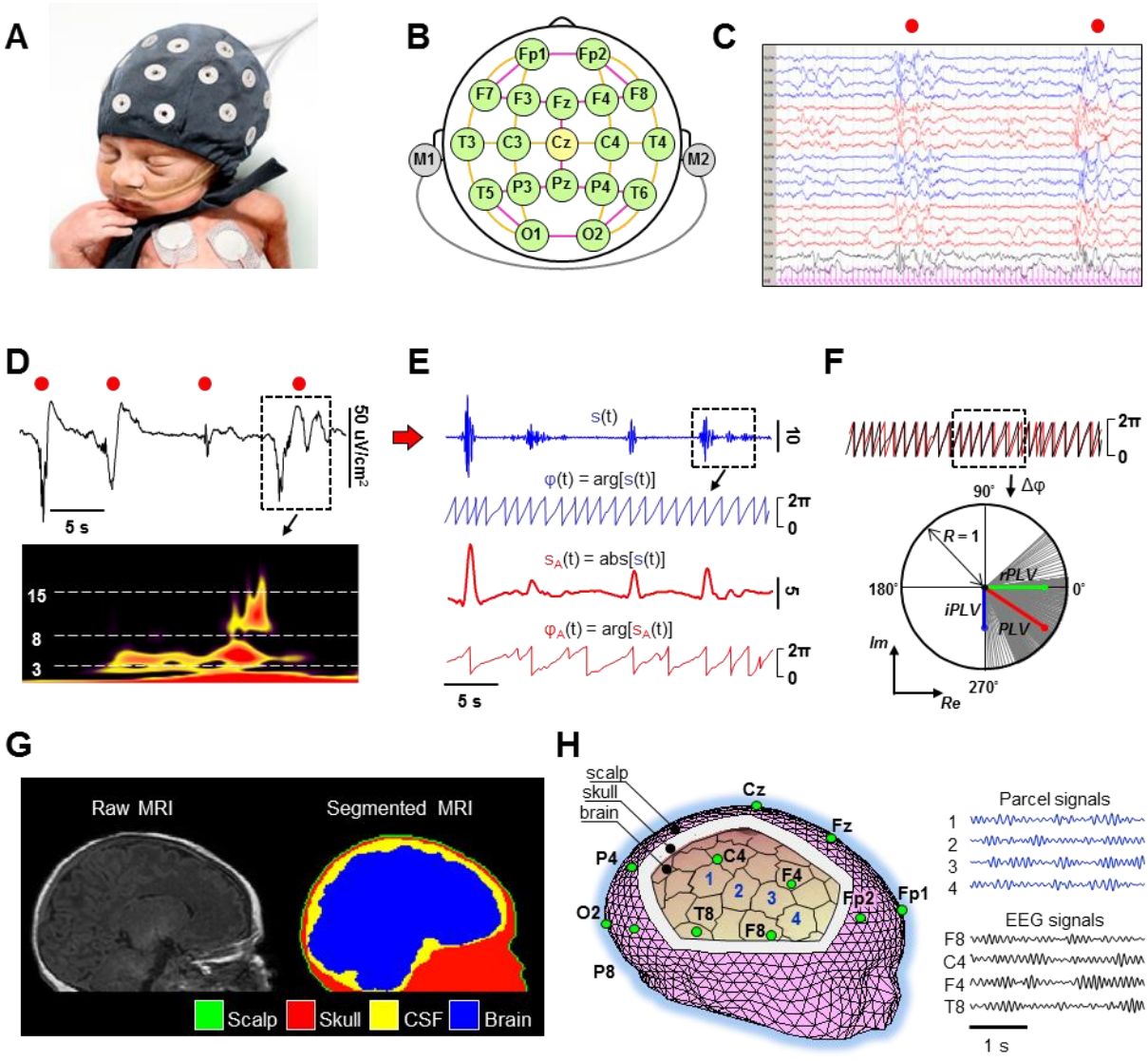

Figure 1. Summary of methods. **A**. High-density EEG recording from an early preterm infant at 30 weeks gestational age (GA). Image courtesy of University of Helsinki, Finland. **B**. The placement scheme of 19 electrodes according to the international 10–20 system. Pairwise combinations for bipolar montages are shown by the orange (banana) and pink (transverse) lines. The monopolar montage with the Cz electrode (yellow) as the common reference is calculated by subtracting the Cz signal from all other electrodes. The linked mastoids reference is computed as an average over mastoid electrodes M1 and M2 (grey). **C**. An example of a multichannel EEG recording from a new-born infant. The red circles indicate the spontaneous activity transients (SATs). **D**. An example of an EEG epoch from an early preterm infant. The red circles indicate SATs, and the wavelet transform for the last SAT (dashed box) is shown below. Note the multi-frequency nature of the SAT events: higher frequency oscillations are nested at a low frequency fluctuation (usually <1 Hz). **E**. Band-pass (3–8 Hz) filtered EEG epoch (shown in D) *s(t)* and its phase function *φ(t)* are shown in blue. The smoothed amplitude envelope $s_A(t)$ and its phase $\varphi_A(t)$ are shown in red. **F**. An example of a phase synchrony estimation. Two phase functions of the band-pass filtered (3–8 Hz) EEG signals are shown at top in red and black. For a fixed time window (dashed box), instantaneous phase difference $\Delta\varphi$ was computed and its distribution over the unit circle appears below. Each grey line corresponds to a phase difference at a certain time point. Phase locking value (*PLV*) reflecting the coherence of this distribution (see also Eq. 11) is illustrated by the red line. Its projections on a real and imaginary axis are estimators *rPLV* and *iPLV*, respectively. **G**. An example of a raw (left) and segmented (right) MRI slice from a healthy full-term infant. **H**. A realistic 3D neonatal head model reconstructed from the segmented MRI is shown on the left. The cortical surface was divided into distinct regions (parcels). The green circles illustrate the location of the EEG electrodes on the scalp surface. At right, examples of simulated parcel (brain) signals are shown in blue and the derived corresponding scalp EEG signals are shown in black.

2.5. Physiological origin of EEG signals

The EEG signal origin is directly related to the basic mechanism of neuronal interaction such as a synapse. The insulating cell membrane electrically separates intracellular space from its environment. Due to an unequal concentration of Na^+, K^+, and Cl^- ions across the membrane (typically, the extra-/intracellular concentrations of these ions for mammalian neurons are 145/15 mM, 5/140 mM, and 110/10 mM, respectively) in the resting state, the intracellular environment relative to the extracellular is negatively polarised (the membrane potential in the resting state is normally about −70 mV).

A synapse is a functional connection between two neurons, making signal transmission between them possible. When an action potential (AP) arrives at the presynaptic terminal of the axon of an active neuron, special molecules called 'neurotransmitters' are released into the synaptic cleft between neurons. These molecules bind to specific transmitter-gated proteins (receptors) located on the postsynaptic terminal of the other neuron. As a consequence of such an interaction, receptors become permeable to the specific ion species. The redistribution of the ions across the cell membrane creates a postsynaptic potential. The influx of positive ions, or cations, (mostly Na^+ and Ca^+) into the cell creates an excitatory postsynaptic potential (EPSP; depolarising the membrane potential and thus increasing the probability of AP generation), whereas the influx of negatively charged ions (Cl^-) creates an inhibitory postsynaptic potential (IPSP; hyperpolarising the membrane potential and thus decreasing the probability of AP generation). The inward flow of cations during EPSP creates a local extracellular 'sink' (a lack of positive ions close to the apical dendrites). At the same time, the redistribution of cations occurs within the neuron. This leads to a depolarisation of the membrane close to the cell body and, as a sequence, to an outward flow of positive ions (return current). This creates an extracellular 'source'. So, the 'sink' (has negative polarity) and 'source' (has positive polarity) form the potential difference that causes an electrical current to flow through the volume conductor. These spatially distinct extracellular fields close to the neuron can be modelled as dipole (Baillet et al. 2001; Lopes da Silva 2004; Hallez et al. 2007; Buzsaki et al. 2012), and they give rise to the potentials measured with scalp EEG.

It is worth noting that despite the undoubtedly major role of EPSPs, currents caused by IPSPs may also lead to the formation of extracellular potentials (Lopes da Silva 2004; Glickfeld et al. 2009; Trevelyan 2009).

One single neuron produces too small electrical potential on the scalp to be detected with EEG (Nunez and Srinivasan 2006). Two crucial factors make 'seeing' neuronal activity at the scalp possible: the structural organisation of neurons in the cortex and the time scale of the extracellular

currents. Pyramidal neurons span multiple cortical layers but the somas of the large pyramidal neurons are predominantly in layer III and V. Neighbouring pyramidal cells are organised such that their dendritic trunks are parallel relative to each other and together lie perpendicular to the cortical surface. Thus, during the activation of the neuronal population, electrical fields from single neurons are summated and the resulting field may be measured by electrodes (Nunez and Silberstein 2000). As long as neighbouring neurons fire with only a slight delay, such a time period allows for their temporal overlap. The proximity of the EEG generators (in the cortex) relative to the scalp is important, because the contribution of the dipole to the scalp potential decays rapidly enough and is inversely proportional to the square of the distance.

To summarise, EEG records the superposition of post-synaptic activity in cortical populations that reach the scalp surface due to volume conduction. This physiological mechanism forms the basis of different mathematical approaches when modelling electrical neuronal activity based on extracranial measurements.

2.6. Neonatal EEG

In contrast to adult EEGs, neonatal EEG features a discrete temporal structure (Buzsaki and Draguhn 2004; Steriade 2006). It is composed of events called SATs (see Figures 1C–D) and the intervals between them (inter-SATs; Vanhatalo et al. 2005a; Vanhatalo and Kaila 2006; Tolonen et al. 2007). Such structures are already visible in EEGs from extremely preterm neonates at about 24 weeks GA (Lamblin et al. 1999; Selton et al. 2000; Vecchierini et al. 2003; Vanhatalo and Kaila 2006) treated in NICU. Studies in animal models report similar patterns for neuronal activity recorded from the cortical structures during early maturation (Khazipov and Luhmann 2006; Sipilä and Kaila 2008).

The presence of SATs represents a key feature of the neonatal EEG making it unique. Researchers suspect that during early development, while the mechanisms for sensory input are not yet established, they play a crucial role in the formation of neuronal connections in the brain (Pallas 2001). SATs represent distinct phenomena from neuronal oscillations generated by the cortex. Several studies highlight the self-organisation of these events in time and in space (Ben-Ari 2001; Sipilä et al. 2005; Khazipov and Luhmann 2006). These events appear in the neonatal EEG during the third trimester and vanish near as full-term GA approaches (Vanhatalo and Kaila 2006). Interestingly, their disappearance concurs with the maturation of the inhibitory GABAergic mechanisms (Dzhala et al. 2005; Vanhatalo et al. 2005a; Vanhatalo and Kaila 2006) required for the regulation of cortical neuronal activity with a high temporal precision (Buzsaki and Draguhn 2004;

Palva et al. 2005). Studies also demonstrated that SATs may be produced both by an isolated cortex (Adelsberger et al. 2005) and by responding to the transient subplate structure inputs (Dupont et al. 2006; Vanhatalo and Kaila 2006).

Prior to reaching full-term, while the inhibitory mechanisms essential for high-frequency activity generation are absent, the signal power of neonatal EEG is mostly concentrated below 30 Hz (Vanhatalo et al. 2005a). By frequency content, SATs are multiband events (Figure 1D). Bursts of higher-frequency activity are packed (or 'nested') within high-amplitude slow waves (<1 Hz) (Vanhatalo et al. 2004; Vanhatalo et al. 2005b; Tolonen et al. 2007). Thus, some literature refers to SATs as *nested oscillations* (Vanhatalo and Kaila 2010).

Spatially, SATs are first (up to 30 weeks GA) visible over the sensory cortices. Animal studies demonstrated this as fibres from the thalamus grow from the subplate into the cortical layer (Penn and Shatz 1999; Price et al. 2006). This corresponds to the idea that brain activity plays a guiding role in the early wiring. Later during development, these events spread over increasingly broader areas (Scher 2005).

During maturation, the power of lower frequencies in SATs gradually decreases. At the same time, higher-frequency activity shows an increase in power and becomes better nested within the slow waves. Towards full-term GA, SATs also become more prolonged and their morphology changes. By comparison, on-going cortical activity (inter-SATs) in early preterm infants is quite insignificant, while closer to full-term, it increases (Vanhatalo and Kaila 2006; Tolonen et al. 2007). The rate of SAT appearance remains approximately the same throughout maturation. This neonatal EEG metamorphosis may be thought of as the gradual increase in on-going cortical activity (inter-SATs) and a decrease in SATs until they completely vanish. In other words, the main trend in EEG alteration during early maturation is from a discontinuous, discrete form towards a continuous, adult-like form. Changes in EEG reflect the physiological and structural changes that take place in the infant brain. The presence of two different trajectories (SATs and inter-SATs) and a progressive change in the balance between them across time indicates the need for mathematical approaches capable of tracking both.

Neonatal EEG also has different features during distinct vigilant or sleep states. During active sleep (AS), features are more continuous and SATs appear more frequently. In contrast, during quiet sleep (QS), the EEG trace is more discontinuous with less frequent SATs (Vanhatalo and Kaila 2006; André et al. 2010; Palmu et al. 2013).

2.7. Extracting neuronal signal attributes

The key parameters of interest for neuronal oscillations include the *amplitude* and *phase* derived from their *complex* representation. The general expression for a complex number *z* is

$$z = a + jb, \tag{1}$$

where *a* and *b* are real numbers called *real (Re)* and *imaginary (Im)* parts, respectively, and *j* is the imaginary unit ($j = \sqrt{-1}$).

Amplitude (*A*) of *z* is computed as

$$A = \sqrt{a^2 + b^2} \tag{2}$$

and phase (θ) as

$$\theta = arctan\frac{b}{a}. \tag{3}$$

In the polar form, *z* can be written as follows:

$$z = A \cdot exp(j\theta). \tag{4}$$

The amplitudes of the signal at each time point form its *amplitude envelope* and the instantaneous phase values form its *phase function* (Figure 1E).

In reality, EEG amplifiers measure the real values of signal *s(t)* and, in this case, information about the amplitude and phase are mixed. There are two commonly used methods to transform measured EEG signals into a complex form. The first applies the Hilbert transform to the signal. This implies computing the convolution of a given signal *s(t)* with function $1/\pi t$ in order to determine the imaginary part of the signal:

$$\dot{s} = s(t) * \frac{1}{\pi t} = \frac{1}{\pi}\int_{-\infty}^{+\infty} \frac{s(\tau)}{t-\tau} d\tau. \tag{5}$$

Because the integral in Eq. (5) is improper, in practice the Hilbert transform is computed as the *Cauchy principal value (P.V.)*:

$$\dot{s} = \frac{1}{\pi}\ P.V. \cdot \int_{-\infty}^{+\infty} \frac{s(t)}{t-\tau} d\tau. \tag{6}$$

As a result, for original signal *s(t)*, we can write *analytic signal* $s_a(t)$ using a complex form:

$$s_a(t) = s(t) + j\dot{s}(t), \tag{7}$$

where *s(t)* is the real part of the signal and *ṡ(t)* is imaginary. As a rule, the Hilbert transform is applied to the band-passed signal in the specific frequency range of interest, but not to a 'raw' signal directly. It is important to remember that the filtering procedure may lead to the distortion of the original phase of a signal. Finite impulse response (FIR) filters introduce a linear phase shift, whereas infinite impulse response (IIR) filters lead to a nonlinear phase shift. Preserving the phase of neuronal oscillations is crucial for analyses such as phase synchrony estimation. Applying any type of filters (FIR or IIR) to a signal in the forward and reverse directions allows us to perform zero-phase filtering (e.g., the original phase function remains 'untouched').

The second alternative for obtaining a recorded EEG signal in a complex form is to apply the continuous wavelet transform. Complex Morlet wavelet $w(t, f_0)$ is widely used for the analysis of neuronal signals (Tallon-Baudry et al. 1997; Lachaux et al. 1999; Palva et al. 2005). Both the imaginary and real parts of this wavelet are essentially harmonic functions windowed by the Gaussian envelope (Kronland-Martinet et al. 1987) well-suited for the analysis of rhythmic neuronal signals such as EEG. The Morlet wavelet is defined as:

$$w(t, f_0) = B \cdot exp\left(\frac{-t^2}{2\sigma_t^2}\right) \cdot ex\,p(2j\pi f_0 t), \tag{8}$$

where $B = \pi^{-1/4}$ is a normalisation factor. The Morlet wavelet has a Gaussian shape both in the time domain with standard deviation (SD) $\sigma_t = m/2\pi f_0$ and in the frequency domain around a central frequency f_0 with SD $\sigma_f = f_0/m$ respectively. Parameter m regulates wavelet resolution both in the time and frequency domains and, in practice, should be set to greater than 5 (Grossmann et al. 1989). The wavelet transform simply refers to the convolution of a signal with the following wavelet function:

$$s_w(t, f_0) = s(t) * w(t, f_0). \tag{9}$$

It is much more efficient to calculate the convolution in the frequency domain. In this case, convolution is simply a product of the spectra obtained with the help of a fast Fourier transform (FFT). The resultant vector $s_w(t, f_0)$ will have a complex form, analogous to an analytical signal (see Eq. 7), where the real part is a band-passed signal *s(t)*.

Previous work has showed that both approaches yield quite similar results for signal amplitude and phase estimation (Le Van Quyen et al. 2001; Bruns 2004). The main difference is that the wavelet-based approach renders the frequency bandwidth manipulation quite challenging because of the time–frequency compromise (*m* parameter should be set to an optimal value). By contrast, the Hilbert transform may be applied to a pre-filtered signal within any frequency band of interest. A

set of properly adjusted filters makes filtering out very narrow band or wideband signal components with unambiguous cut-off frequencies possible depending on the purpose of the study.

The phase function of the amplitude envelope is extracted similar to neuronal oscillations using the Hilbert transform (see Figure 1E) as was done with original neuronal oscillations.

2.8. Methods of synchrony analysis

Currently, many different approaches to assess synchrony between neuronal oscillations exist. Some metrics take into account both the amplitude and phase of signals. Among them, the most popular include such estimators as the cross-correlation and coherence and their different implementations (Kuks et al. 1988; Grieve et al. 2008; Milde et al. 2011; Witte et al. 2011). The amplitude of neuronal oscillations is believed to reflect the synchronisation of neurons in the local cluster (Varela et al. 2001). This is proportional to the number of co-activated cells in the neuronal population. In turn, phase synchrony is considered crucial for the coordination of activity between distributed neuronal assembles (Fries 2005; Womelsdorf et al. 2007; Lakatos et al. 2008; Uhlhaas et al. 2009; Palva and Palva 2012). Previous reports indicated that amplitude correlation and phase synchronisation between neuronal oscillations relate to functionally different mechanisms (Bruns et al. 2000; Freunberger et al. 2009; Palva et al. 2010; Engel et al. 2013). Moreover, neonatal EEG is typically characterised by a high amplitude variability, making the coherence estimate an amplitude covariance measure (Vanhatalo and Palva 2011).

The relationship between the amplitude envelopes of neuronal oscillation in the simplest case may be assessed by computing the correlation coefficient. Several improved implementations of this approach work with normalised (Bruns et al. 2000) or orthogonalised (Brookes et al. 2012; Hipp et al. 2012) envelopes. These measures may be efficiently used when applied to cortical source signals (Palva and Palva 2012). However, when dealing with EEG recordings, the amplitude estimates of the underlying neuronal activity generators may be biased due, for example, to a change in the dipole orientation relative to the electrodes. Thus, synchrony measures which rely solely on the phase of signals may provide more robust estimates of functional connectivity when dealing with EEG.

Phase synchronisation (PS) between two neuronal signals means that their phase difference ($\Delta\theta$) is stable over a certain period of time. The most common way to assess PS is to compute the phase locking value (*PLV*) between band-passed oscillations within an optimal time window (Jervis et al. 1983; Lachaux et al. 1999; Lachaux et al. 2000; Mormann et al. 2000). For two discrete

signals with phase functions θ_1 and θ_2, respectively, and k as the sample index, the phase difference can be written as:

$$\Delta\theta(k) = \theta_1(k) - \theta_2(k). \quad (10)$$

Then, the *PLV* measure in complex form (cPLV; Aydore et al. 2013) can be written as:

$$cPLV = \frac{1}{N}\sum_{k=1}^{N} exp\left(j\Delta\theta(k)\right), \quad (11)$$

where N is the number of samples within the time window for which the synchrony is estimated, k is the sample index, and j is the imaginary unit. Then, 'classical' *PLV* (Lachaux et al. 1999) can be computed as an absolute value of *cPLV* (see also Figure 1F), ranging from 0 (when the phase difference is uniformly distributed) and 1 (perfect phase stability).

Volume conduction results in the same cortical generator possibly contributing to spatially close EEG sensors, yielding artificial phase synchronisations at the electrode level (Nolte et al. 2004; Tognoli and Kelso 2009; Palva and Palva 2012). Signals related to the same neuronal source usually have zero-phase lag. Several metrics are available that ignore zero-phase lags (Stam et al. 2007; Vinck et al. 2011). These measures are more robust to undesired effects caused by volume conduction but, at the same time, do not capture true neuronal interactions with a close-to-zero phase difference. In this work (see **Study III**), we used the imaginary part of *cPLV* (*iPLV*) for EEG sensor-level synchrony analysis, which only accounts for the non-zero phase differences of the analysed signals (shown in blue in Figure 1F). For the synchrony estimation between the source signals, we applied the real part of *cPLV* (*rPLV*) (shown in green in Figure 1F), taking into account zero-phase lags between neuronal oscillations.

A separate class of measures also allow us to establish a causal relationship between the activities in populations by assessing the information flow between them. These include the Granger causality (Granger 1969), dynamic casual modelling (Friston et al. 2003; Penny et al. 2009), transfer entropy (Schreiber 2000) and phase transfer entropy (Lobier et al. 2014).

Recently, several novel methods such as orthogonalised partial directed coherence (Omidvarnia et al. 2014a) and activation synchrony index (Räsänen et al. 2013) were introduced for the analysis of connectivity in the neonatal EEG. There is still a lack of methods suitable for analysing functional connectivity in a manner that accounts for the coexistence of SATs and the ongoing cortical activity that together form the unique mixture of spontaneous activity mechanisms in the EEG of early preterm infants. Traditionally, the visual assessment of event co-occurrence was

widely used to evaluate maturational changes or abnormalities (Hahn and Tharp 1990; Walsh et al. 2011).

2.9. Mathematical head model

In the context of EEG, the *forward problem* implies the computation of scalp potentials recorded by sensors for a determined configuration of neuronal electrical activity sources (Musha and Okamoto 1999; Mosher et al. 1999; Kybic et al. 2005; Hallez et al. 2007; Wendel et al. 2009). The solution to the *forward problem* is referred to in the literature as a *head model* or *forward solution*. Sources (or current dipoles) at the cellular level refer to the clusters of cortical pyramidal cells. Positions and orientations of both sensors (signal or channel space) and sources (source space) in the model are predefined. The source locations and orientations are derived based on the anatomical data and tightly linked to the geometry of the cortical layer (either the outermost cortical surface or the white/grey matter boundary is usually taken as a source space). The 3-D coordinates of EEG electrodes can be defined empirically from a real human recording, or by positioning the electrodes according to the international system based on anatomical landmarks.

Currently in neuroimaging there are two powerful numerical methods widely used to compute the head model: the Finite Element Method (FEM) and the Boundary Element Method (BEM). The FEM approach was developed in the 1950's (for the history of the development and major contributors see Cheng and Cheng 2005; Hsiao 2006) and the BEM was introduced later in 1970's (Clough 2004). Both methods deal with solving the partial differential equations that model electrical currents from neuronal populations (Gençer and Tanzer 1999; review by Hallez et al. 2007; review by Wendel et al. 2009). The major difference between FEM and BEM is that the first one solves the unknowns for a chosen region of space and requires boundary conditions. In contrast, the latter one solves the unknowns only on the boundaries. In practice, the 3-D objects in FEM have to be discretized with 3-D units (in the simplest case, cubic elements with eight nodes), while for BEM it is enough to model boundaries (shells) with 2-D elements. Consequently, the computational load of BEM is lighter compared to FEM. To reduce further the computation of the *head model* using BEM, shells are usually down-sampled to a sparser tessellated grid (from the triangle elements in most cases). The optimal size of the triangle edges for the folded cortical surface approximation is about 5-7 mm (Fischl et al. 2001; Segonne et al. 2007). Other smoother tissues can be approximated using even larger triangle elements. The main disadvantage of the BEM approach is that all tissues are assumed to have homogeneous and isotropic (the same in all directions) conductivity. In reality, some head tissues, such as white matter and the skull, have anisotropic

conductivity (directional dependence). From this point of view, the FEM model is potentially more realistic because the anisotropic properties of the tissue can be taken into account. In the case of neonatal head modelling, the FEM technique can take into account the effects of fontanels as well.

The accuracy and performance of the model strictly depends on the accuracy of the tissue layer geometries, on the proper conductivity values selected for them, as well as on the fidelity of the solver (Hämäläinen and Sarvas 1989; Ramon et al. 2006b; Cho et al. 2015). Realistic boundaries for the major head tissues (scalp, skull, cerebrospinal fluid (CSF), white and grey brain matter) are reconstructed from anatomical magnetic resonance images (MRI, Figure 1G) of the head. Recent studies have introduced several head models with a higher number of head tissue compartments (Ramon et al. 2006a; Irimia et al. 2013). At present, many different implementations of the BEM (Hämäläinen and Sarvas 1989; Musha and Okamoto 1999; Frijns et al. 2000; Fuchs et al. 2001; Akalin-Acar and Gençer 2004; Gramfort et al. 2010) and FEM (Yan et al. 1991; Haueisen et al. 1995; Wolters et al. 2002; Gençer and Acar 2004; Ramon et al. 2006b) solvers exist.

An opposing problem focused on how to reconstruct the cortical source activity from the scalp EEG signals is referred to as the *inverse problem* (see review by Grech et al. 2008) which requires a forward solution. In the literature, *source localisation* refers to solving both *forward* and *inverse* problems, resulting in a set of estimated time series related directly to the cortical electrical activity generators.

2.10. Current state of neonatal head modelling

A realistic and reliable head model is a key requirement for the plausible forward simulation of the scalp potentials as well as for the accurate estimation of the neuronal electrical activity at the source level. This is also important for accurate source reconstruction from electrical potentials on the scalp. In recent years, interest in source localisation techniques applied to infant EEG increased. The analysis of neuronal electrical activity at the source level provides more physiologically relevant information which is less biased by volume conduction effects. Several studies used source reconstruction methods to localise generators of evoked-response potentials (ERP) in several months old infants for visual attention and recognition memory (Reynolds and Richards 2009) and auditory processing (Hämäläinen et al. 2011; Ortiz-Mantilla et al. 2012; Musacchia et al. 2013). Another study analysed pathological and physiological electrical activity in newborns using source localisation of focal EEG transients (Roche-Labarbe et al. 2008). The usefulness of this approach to successfully localise seizures in the same age group has been demonstrated (Despotovic et al. 2013).

Currently, several technical issues and theoretical knowledge gaps exist pertaining to the complexity of neonatal head geometry, thus preventing the wide application of source localization. Realising that a neonatal head model is not only different in size compared to an adult is important. The reliable forward solution requires accurate geometry of the head tissues, which is usually obtained by segmenting the subject's anatomical MRI. Several algorithms exist for automated tissue classification from a neonatal MRI (Prastawa et al. 2005; Weisenfeld and Warfield 2009; Shi et al. 2010), however automated segmentation has proven difficult and less reliable than the time-consuming manual tissue segmentation. Moreover, the resolution of most MRI scanners is quite low for quality neonatal tissue sampling. Thus, in some cases, an anatomical MRI undergoes interpolation (Despotovic et al. 2013) potentially distorting the real geometry. Additionally, individual anatomical data are rarely available for subjects. Some studies overcome this by applying data from a single subject to an entire group (Reynolds and Richards 2009), using age-appropriate brain templates (Hämäläinen et al. 2011), or simply rescaling adult anatomy (Jennekens et al. 2013). Some studies showed that more accurate results can be achieved using realistic individual head models (Roche-Labarbe et al. 2008; Song et al. 2013; Despotovic et al. 2013).

The segmentation of a structure such as the fontanel remains challenging (Despotovic et al. 2013; Lew et al. 2013). Recently, initial efforts to automate fontanel segmentation were completed (Jafarian et al. 2014). Also, the conductive properties of tissue in the neonatal head are distinct from adults and change with age. The most crucial point is to account for proper skull conductivity in the model since this represents the major cause of neuronal electrical signals attenuation (Hallez et al. 2007). At the moment, no reasoned value for the neonatal skull exists. Thus, in most models, this value is normally set to an adult value, extrapolated from the data available for older children (Hämäläinen et al. 2011) or varied between theoretically possible extremes (Roche-Labarbe et al. 2008; Despotovic et al. 2013). In addition, because of the quite extensive structural changes in the neonatal head, structural (MRI) and functional (EEG) data should be measured from a single subject relatively closely in time. Finally, no existing approaches accounting for the contribution of the subplate structure during early maturation in EEG signals exist.

3. AIMS

The primary goal of this Thesis focused on developing mathematical approaches to assess the functional connectivity during maturation starting from an early preterm age. The specific aims were to:

- Develop an algorithm capable of assessing functional connectivity based on events and oscillations in early preterm (GA 27–31 weeks) infants (**Study I**).

- Estimate the realistic value of skull conductivity in infants and to study the spread of neuronal electrical activity within the neonatal head (**Study II**).

- Investigate the influence of the EEG recording montage settings (the number of electrodes and reference) on phase synchrony estimates in infants (**Study III**).

4. METHODS

4.1. Data acquisition

We completed high-density EEG (hdEEG) recordings of preterm and full-term infants using individually attached electrodes as well as specially designed neonatal EEG caps (Figure 1A; Vanhatalo et al. 2008; Stjerna et al. 2012). In **Study I,** we varied the number of electrodes from 20 to 28, while in **Study II** we used 64 electrodes. We recorded adult EEG signals for **Study II** using 128 electrodes. We measured EEG signals with the sampling frequency (*Fs*) equal to 512 Hz (**Study I**) and 256 Hz (**Study II**). Further details about acquisition systems, recording procedures, and subjects are in the original publications.

For the 3-D infant head model reconstruction in **Studies II** and **III,** we used a set of anatomical MRIs (176 slices in total) from a healthy full-term neonate (Figure 1G).

In **Study I,** we used clinical brain ultrasound images for infants with lesions in order to assess the spatial performance of the proposed EEG-based algorithm.

4.2. Signal pre-processing

In all studies included in this Thesis, we used artefact-free EEG epochs for the analysis. In **Study I,** EEG signals were filtered using a set of seventh-order Butterworth filters to bands 0.25–3 Hz, 3–8 Hz, 8–15 Hz and 15–30 Hz. Zero phase shift was achieved by applying the filters both forward and backward in time. Subsequently, we applied the Hilbert transform to these filtered signals, resulting in a complex-valued analytical signal. We then used these to extract phase functions and amplitude envelopes for further connectivity analysis. Amplitude envelopes (band amplitude fluctuations or BAFs) associated with SAT events were also smoothed using the Savitzky–Golay method (Savitzky and Golay 1964) and high-pass filtered to remove any infra-slow components using a seventh-order Butterworth filter with a cut-off frequency of 0.1 Hz. Next, we extracted the phase functions of the amplitude envelopes analogously using the Hilbert transform. In **Study II,** in order to remove slow components from the EEG data, we used a median filter applied to a 230-ms time window. In **Study III,** we simulated neuronal activity from cortical areas by applying a Morlet wavelet filter to white noise (centred at 10 Hz and with parameter *m* defining the time–frequency trade-off set to 5). This led to a set of simulated complex-valued narrow-band signals.

4.3. Connectivity analysis

For the phase synchrony analysis between scalp EEG signals from preterm infants, we used the *PLV* measure. We applied this to assess functional connectivity at both temporal levels: band-passed oscillations and their amplitude envelopes. In the first case, we computed *PLV* in a sliding frequency-specific time window (for example, see Figure 1F). Window length was equal to the duration of the six cycles at the central frequency of the analysed range. We tested the significance of *PLV* with the help of surrogates (in total, 200 for each signal pair). We divided one of the signals into discrete time-windows. We then shifted in time these time-windows 200 times, creating 200 surrogate time-series. We then computed *PLV*s between intact EEG and each of surrogates. We estimated the event-level synchronisations in an analogous manner. We set the time window for *PLV* to 4 s for all BAFs. We created the set of surrogate values by computing *PLV* for all possible combinations between the BAF pairs tested during the 4-s time window. In both cases, we set the significance level to 0.05.

In the simulations of cortical activity and its reflection on the neonatal head, we used two different synchrony measures: the imaginary and real parts of complex *PLV* (*iPLV* and *rPLV*, respectively; see Figure 1F). We estimated the synchrony between the original brain signals and EEG scalp signals using *rPLV*, because no phase shift was present in this case. When we introduced coupling using a phase delay between two random cortical regions, we estimated the synchrony at the electrode level using *iPLV*. Doing so reduced the number of spurious couplings between scalp electrode signals caused by volume conduction. Additional details about connectivity estimation and statistical testing of its significance can be found in the articles corresponding to the work presented in this Thesis (**Study I** and **III**).

4.4. Generating baby head models

For a neonatal 3-D head reconstruction (Figure 1H), we used a set of anatomical MRIs. In total, we used 176 slices in the stack with a slice thickness of 0.9 mm. Each slice had a dimension of 240 × 256 pixels with a pixel resolution of 1 × 1 mm^2. In order to yield a maximally realistic and precise geometry of the head tissue, we segmented the MRI data manually (Figure 1G). All MRIs were segmented into five compartments: scalp, skull, CSF, brain, and eyes. For the FEM model, we used all compartments, whereas for the BEM the eyes were not needed.

We computed the FEM head model using the approach reported by Ramon and colleagues (2006a). This method works by approximating the tissue volumes using discrete cubic elements with an edge size varying from 1 to 16 mm. We computed the forward solution for all scalp points

(in total, 90 649 points). To compute the BEM head model, we used the symmetric BEM algorithm (Kybic et al. 2005; Gramfort et al. 2010). We approximated the outer boundaries of the scalp, skull, and CSF using tessellated grids each containing 2562 vertices. The cortical surface was taken as the source space and represented by a mesh of 4322 vertices (the distance between neighbouring sources was about 3 mm) each corresponding to a cluster of active neurons. In **Study II,** we computed the forward solution for each vertex of the triangle mesh representing the scalp. In **Study III,** however, we computed the forward solution for different sets of electrodes (from 11 up to 85) placed on the scalp surface according to the international 10–20 system.

We used the conductivity values for the brain, CSF, and scalp compartments from previous studies (Ramon et al. 2006b; Roche-Labarbe et al. 2008; Despotovic et al. 2013) setting them to 0.33 S/m, 1.79 S/m, and 0.43 S/m, respectively. Since the central problem in **Study II** included the empirical assessment of neonatal skull conductivity value, we tested different values: 0.0033 S/m, 0.033 S/m, and 0.33 S/m. Based on results of **Study II**, we performed the simulations in **Study III** using conductivity values 0.2 S/m and 0.033 S/m for the neonatal skull in the BEM model.

In **Study II** for both the FEM and BEM approaches, a single source was active at the time, whereas all others remained silent. We tested sources located at different depths within the head with the amplitudes uniformly set. In **Study III,** all sources in the cortex remained active throughout, with their activity (source signals $s_s(t)$) modelled as white noise filtered using a Morlet wavelet centred at 10 Hz. We derived scalp EEG signals (or electrode signals $s_e(t)$) as a product of the forward solution and source signals (see also Figure 1H):

$$s_e(t) = F \cdot s_s(t), \tag{12}$$

where F is a forward solution (matrix with the dimensions of the number of electrodes by the number of sources).

It is noteworthy that, in **Study III,** we preferred using the BEM model over FEM due to its simpler implementation and better computational efficiency. In cases when accounting for anisotropic properties of tissue conductivities is unnecessary, both methods yield quite similar results. Research has also shown that the fontanel (implemented only in the FEM model) carries a minor effect on the estimation of neuronal electrical activity spread within the head (Despotovic et al. 2013).

5. RESULTS

5.1. Event synchrony as a marker of structural abnormalities (I)

In the context of this Thesis, we proposed a new algorithm for synchrony assessment in preterm infants. This new algorithm was designed to estimate functional connectivity at two different scales: the band-pass filtered neuronal oscillations and their amplitude envelopes corresponding to SAT event appearance. This method was designed to work with multichannel EEG recordings making spatial mapping of the functional connectivity in neonates possible. The signal pre-processing steps and the parameters for synchrony analysis underwent data-driven optimisation to maximally fit the specific EEG features for early preterm infants. Further details related to the technical aspects of the algorithm may be found in the corresponding article (**Study I**) upon which this Thesis is based. We evaluated the efficiency of the approach using real multichannel clinical EEG recordings from healthy preterm infants and from infants with brain lesions.

One important observation is that we found no laterality at both temporal scales in the functional connectivity in healthy infants. We also found no significant differences in the phase synchrony between groups at the level of neuronal oscillations. In turn, we observed a statistically significant reduction in the event-level synchrony in sick infants compared to healthy subjects. We detected those functional disruptions in multiple frequency bands and at different locations.

We found that the long-range interhemispheric event-level functional connectivity in infants with brain lesions was significantly lower at the frontal and parietal locations in the 8- to 15-Hz frequency band, while it was lower in the central location within the 3- to 8-Hz frequency band. We observed a decrease in the short-range local intrahemispheric synchrony in many frequency bands, primarily around the central and lateral parietal derivations. Additional details about the spatio-frequency differences between the groups are shown in Figure 2A.

We also compared groups of infants using alternative measures such as the root mean square (RMS) of the signal, number, and cumulative fraction of SATs (SAT# and SAT% respectively, see also Palmu et al. 2010a; Palmu et al. 2010b). We found a significant difference between sleep (AS vs. QS) states using such estimators in healthy infants.

5.2. Neonatal skull conductivity revised (II)

In the context of this study, we created two infant head models using two different methods: BEM and FEM. We used both methods to simulate the electrical activity of the cortical source and its spread within the neonatal head. By manipulating the skull conductivity value in the head models

and then comparing the spread of electrical potentials on the scalp surface with the amplitude decays in real EEG data, we empirically estimated its meaning.

We found that in infants EEG amplitudes decay quite rapidly within a few centimetres of the reference electrode. A correlation analysis of the transients between different channels showed the same tendency. This effect was independent of electrode location and consistent across subjects. This decay in neonates was about three times faster than that in adults. Simulations of the cortical activity using two head models showed how quickly the real data decays when the values of the skull conductivity were set to within 0.06 to 0.2 S/m of the diapason (see Figure 2B). To summarise, in the neonatal head, the nature of the cortical activity spread towards the scalp is more confined than that in adults due to the higher conductive properties of the skull at that age.

5.3. Influence of the EEG montage on the connectivity analysis (III)

Our mathematical simulations using a realistic neonatal head model showed that an increase in the number of scalp electrodes leads to a systematic improvement in the detection of the cortical signals as well as an increase in the amount of useful information about brain activity. This effect remained independent of the reference in the montage. The maximal number of observed cortical sources refers mostly to the relationship between the cortical area size that produces the neuronal oscillation and the inter-electrode distances in the recording sensor array. The performance of the high-density electrode mesh worsens, however, when the number of active brain parcels increases without any significant changes in their size. The amount of non-redundant information in EEG recordings also relates to the size of the scalp area covered by sensors. In terms of functional connectivity analysis, dense electrode arrays improve spatial mapping, but are also associated with an increasing number of spurious couplings between EEG signals. This effect can be minimised through properly choosing the reference in the montage (Figure 2C).

Our results show that montages with a grand average reference and CSD transform carry a greater robustness to cortical signal smearing at the scalp surface as well as a better specificity and sensitivity in the source coupling detection compared to conventional montages. The performance of these montages is highly dependent on the number of electrodes in the recording array. The CSD montage is also sensitive to spatial smoothing, which is traditionally used to improve its performance when the sensor mesh is sparse. Smoothing severely diminishes the fidelity of CSD even with high-density arrays. We also demonstrated that the most accurate registration of true cortical signals is possible when using CSD montage. We found that the montage with the common Cz reference was most sensitive to volume conduction.

We also tested the widely-used clinical EEG recording protocols comprising only 19 electrodes using different variations of bipolar or monopolar derivations or linked mastoids as the reference point. All showed moderate performance mostly due to the low electrode number. Still, the global average and linked mastoid montages showed the best recording quality and robustness to volume conduction. The performance of CSD was slightly worse, while we obtained the worst results using the monopolar montage.

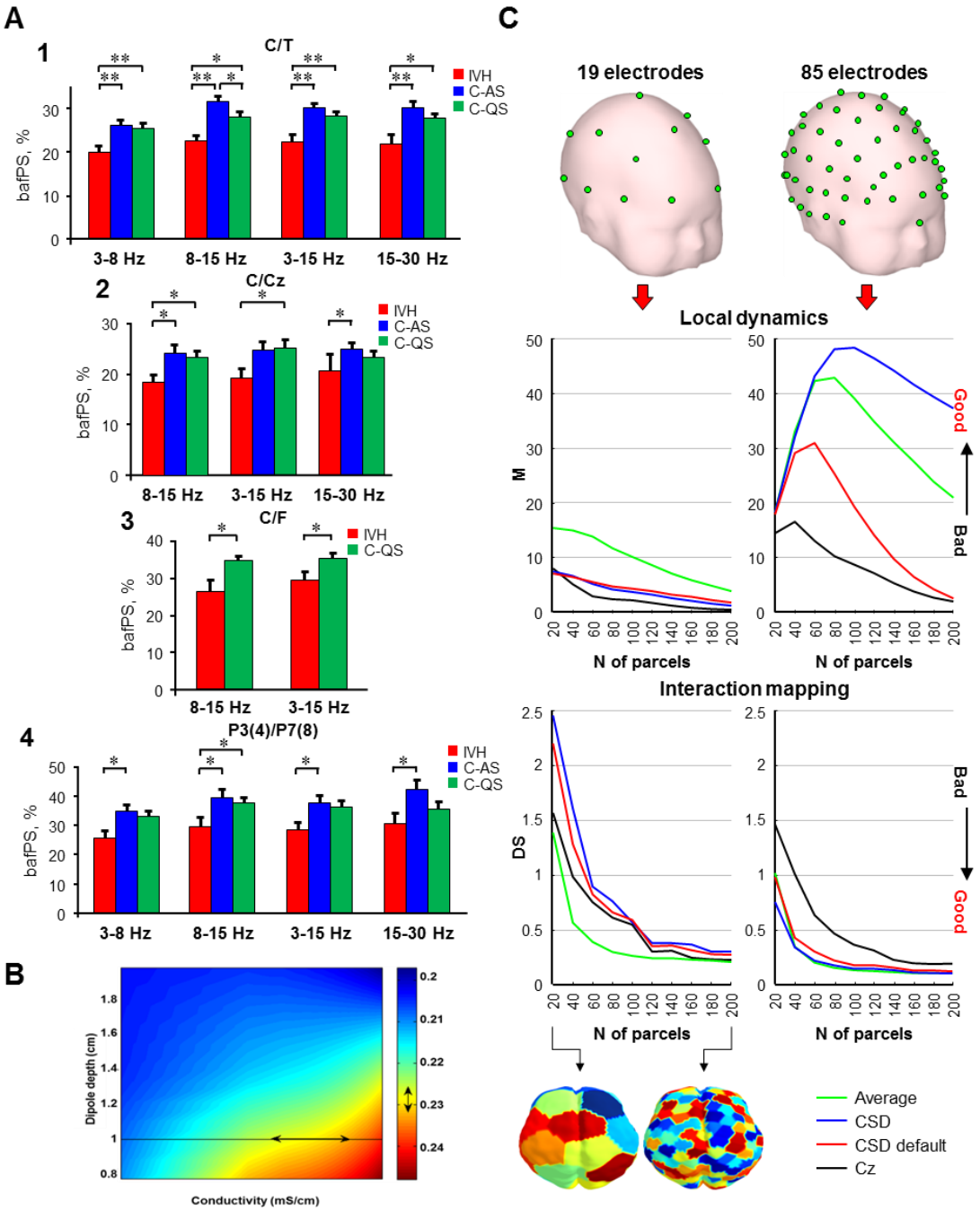

Figure 2. Selected results. **A**. Event-level synchrony difference between control groups during active sleep (C-AS) and quiet sleep (C-QS) versus infants with intraventricular haemorrhage (IVH). The gestational age (GA) of the subjects was 27 to 30 weeks. A comparison of groups demonstrates that IVH infants exhibited significantly lower local band amplitude fluctuation phase synchrony (bafPS) at multiple frequency bands around the central derivation (A1–3), as well as in the lateral parietal connections (A4). Bars indicate the average values for neonatal groups; error bars show the standard error of the mean (SEM) values; $*p < 0.05$. $**p < 0.01$. Wilcoxon test. **B**. Summary of all simulation results (see **Study II** for further details) combining skull conductivity (X axis), source (dipole) depth (Y axis), and the slope of the spatial amplitude decay (Z axis). These limit the yield of the suggested range of infant skull conductivities at around 0.06 to 0.2 S/m. **C**. The fidelity of the montages with 19 (left column) and 85 (right column) EEG electrodes. The upper graphs compare the ability of different montages (the colour key is shown at the bottom right corner of the figure) to detect the local dynamics estimated with the maximal number of cortical details (or parcels, M) that the montage can detect. Note the dramatically increased number of discernible cortical parcels using a higher number of recording electrodes. The lower graphs compare the level of spatial smearing of coupled brain signals at the electrode level (measured using a degree of smearing estimator, DS) with each montage. Note how the spatial smearing is clearly lower with a higher number of electrodes. However, clear differences between the montages also exist. Taken together, the results suggest that the average reference is generally better with a lower number of recording electrodes, while the CSD montage improves when the recorded electrode count is higher. For technical details regarding the fidelity estimators used to validate the EEG montages, please see **Study III**.

6. DISCUSSION

6.1. Synchrony assessment in preterm infants

Synchrony analysis applied to neonatal EEG signals represents a relatively easy way to track the wiring processes in the infant brain during early maturation. Proper wiring in the neonatal brain strongly relies on its own endogenous neuronal activity (Smyser et al. 2010). Changes in connectivity may be assessed using various synchrony estimates. Neonatal EEG at an early preterm age up to a few months after reaching full-term features a discrete temporal structure that comprises SAT events and inter-SAT intervals. Two distinct physiological mechanisms stand behind such a configuration, both of which are important for the establishment of brain networks (Vanhatalo et al. 2005a; Tolonen et al. 2007; Omidvarnia et al. 2014b). SATs play an important role in early neuronal wiring and guide the functioning as the internal reference (Vanhatalo and Kaila 2006; Vanhatalo and Kaila 2010). Changes in SAT synchronisation may be evaluated through the analysis of couplings between amplitude fluctuations of the band-pass filtered EEG signals (that is, BAFs). During maturation, when sensory inputs become available, this mechanism gradually vanishes. The wiring then is mostly driven by external information and changes in coupling strengths are more likely detected between pure oscillations within certain frequency bands (Feller and Scanziani 2005; Blankenship and Feller 2010; Hanganu-Opatz 2010; Espinosa and Stryker 2012; Colonnese and Khazipov 2012).

The direct application of the commonly used approaches for the analysis of functional connectivity to neonatal EEG will more likely lead to biased results and, as a consequence, mislead interpretations of physiological changes. We proposed a novel method based on the PLV measure for synchrony assessment in infants on both levels: pure oscillations and events. Methodologically similar pipelines of signal processing make tracking synchrony changes simultaneously possible at two different temporal scales. Such an algorithm becomes applicable in the analysis of EEG signals in infants beginning at an early preterm age up to several months after full-term. The parameters in the algorithm were tuned to the specific time–frequency features of EEGs from preterm neonates. Moreover, the computational load of the algorithm was optimised to enable its efficient use for the online clinical monitoring of infant brain activity.

6.2. Brain lesions affect functional connectivity

We used the developed algorithm for synchrony estimation in two groups of preterm infants: healthy infants and infants with vascular brain lesions of different grades and locations. Our results showed a statistically significant reduction to the event-level synchronisation in infants with lesions

compared to the healthy controls. The observed differences were frequency selective (Figure 2A). This result supports the idea that brain lesions, depending upon their size and location, may selectively disturb SATs at multiple frequency bands. Spatially, the primary synchrony difference between groups predominantly appeared in the centro–parietal areas. Previous animal studies reported the important role of these regions for networking during the developmental time window corresponding to the age of the infants we studied (Meyerson 1968; Yang et al. 2009; Marcano-Reik et al. 2010). A brain lesion may lead to connection disordering and, consequently, to the suppression of functional connectivity between these cortical areas.

Importantly, we found this synchrony difference between sick and normal infants irrespective of the vigilance states (active or quiet sleep) associated with the different frequency for SAT appearance (Paul et al. 2003; Palmu et al. 2010a; Palmu et al. 2010b). This also means that distinguishing between sleep states is unnecessary when using the proposed algorithm, which often relies on compromised criteria and may require manual control. This algorithm may be applied directly to unclassified EEG epochs.

We found no significant difference between groups in synchrony at the level of pure neuronal oscillations. We expected this finding, since in preterm infants the brain networks are just growing (Judas et al. 2005; Kostovic and Jovanov-Milosevic 2006) and have not yet established precise connections to support information transfer with the necessary temporal accuracy. Other studies have demonstrated that significant coupling by phase synchrony between EEG oscillations can be seen later when infants approach full-term (Gonzalez et al. 2011; Tokariev et al. unbublished). It is possible, albeit not yet directly studied, that higher frequencies are coupled in early brain networks via nested oscillations, a.k.a. phase–amplitude correlation, which refer to cross-frequency interaction where the amplitude of the fast oscillation is correlated with the phase of the slower oscillation (Canolty and Knight 2010). They may be an essential systems-level mechanism for integrating and regulating large-scale neuronal processing distributed over several frequency bands (Vanhatalo et al. 2005a; Canolty and Knight 2010; He et al. 2010; Monto 2012; Engel et al. 2013), and they warrant future studies in the human preterm EEG.

In addition, we found no significant difference between healthy controls and sick infants using alternative measures (RMS, SAT#, and SAT%) that relate more to the duration and frequency of SATs appearing rather than to their synchronisation. Our results suggest that early in the preterm period among healthy infants event-level synchronisation of neuronal oscillations is a dominant mechanism for the interplay between brain areas. We also found that the functional connectivity approach may be effectively used to noninvasively detect abnormalities that affect early networking during maturation in preterm infants whose brains are still poorly wired.

6.3. Future directions in synchrony analysis

Our algorithm does not distinguish between SAT and inter-SAT episodes in neonatal EEG (Tolonen et al. 2007), but instead estimates the synchrony using an entire epoch. On the one hand, using existing event detectors to separate these distinct types of activity is unnecessary (Vanhatalo et al. 2005a; Palmu et al. 2010a; Palmu et al. 2010b). Despite their reliability among preterm infants, their temporal resolution requires improvement. On the other hand, evaluating synchrony at both temporal levels within SATs and inter-SATs separately is highly interesting and may lead to new insights into the underlying physiological mechanisms and dynamics of early networking in the human brain. In theory, our algorithm may be easily combined with event detectors for such analyses.

It is also well known that synchrony estimates at the level of the scalp electrodes may be strongly biased by volume conduction effects (Stam et al. 2007; Haufe et al. 2013). Studies among adults showed that the analysis of functional connectivity at the source level is more promising than at the level of EEG signals (Schoffelen and Gross 2009; Palva et al. 2010). Reconstructed cortical signals remain less sensitive to volume conduction and amplitude estimates are more accurate since they do not depend on source orientation relative to the EEG sensors. Analysis of the interactions between neuronal activity generators in the brain is also more relevant physiologically. The first attempts at source modelling in neonates have been completed (Roche-Labarbe et al. 2008; Despotovic et al. 2013). In this context, the application of our algorithm to the reconstructed cortical signals makes more sense. In turn, the fidelity and reliability of the source reconstruction strictly depend on an accurate and realistic head geometry (Hämäläinen and Sarvas 1989; Buchner et al. 1997), properly setting the tissue conductivity values (Gençer and Acar 2004; Ramon et al. 2004), and the use of high-density sensor arrays during EEG registration (Hassan et al. 2014).

6.4. Highly conductive infant skull

The adult human skull features roughly one order lower conductivity compared to the surrounding scalp and CSF, and acts as a low-frequency spatial filter (Hallez et al. 2007). Signals from brain sources moving towards the scalp surface mix within the more conductive intracranial space and, then, severely attenuate due to the skull. The skull strongly influences the degree of brain signal mixing and the scale of signal spread over the scalp. It is worth noting that the skull on its own would not cause smearing. This effect is due to the significant difference between the conductivities of head tissues (poor skull conductivity and good scalp conductivity). The neonatal head (including the brain) does not represent a miniature copy of an adult's. It undergoes dynamic

physiological changes and all of its tissues possess different properties that gradually change over time. We analysed real EEG data in combination with computational simulations using realistic neonatal head models (both BEM and FEM) to empirically estimate infant skull conductivity.

Our results show that the conductivity of the neonatal skull tissue is much higher (about 0.06–0.2 S/m; see also Figure 2B) than an adult's (0.0067 – 0.015 S/m; see Oostendorp et al. 2000; Akhtari et al. 2002; Gutierrez et al. 2004; Lai et al. 2005), and approaches the values found in soft tissue (CSF and scalp). The higher conductivity properties in an infant's head result in a focal spread of electrical cortical activity towards the scalp. In contrast to an adult's, a neonatal EEG is characterised by a more rapid spatial decay. The degree of cortical signal mixing at the scalp electrodes varies inversely proportional to the ratios of tissue conductivities (a head model with a skull conductivity of 0.2 S/m lower compared to a model with a 0.033 S/m conductivity). More conductive pathways towards the electrodes in the neonatal head reduce the distribution area of the cortical signals mainly in the skull and scalp compartments. Consequently, the degree of signal mixing decreases.

Our findings fit logically with histological studies of the neonatal skull. Clear evidence shows that a newborn's skull bone is not yet ossified and its properties remain different from an adult's (Ernst 2011). Our results may be applied to improve infant head models used for forward simulations as well as for cortical source reconstruction.

6.5. Fontanel not a privileged path for electrical activity

The fontanel, a specific structure of the neonatal skull, includes membranous gaps in the cranial bones. Immediately following delivery, the fontanel remains small in infants. During the first months of life, these gaps become larger and, then begin closing with maturation (Erasmie and Ringertz 1976). Accounting for this structure in the neonatal head model presents challenges and increases the model's complexity. In FEM models, the fontanel is usually considered a distinct segment that must be extracted from anatomical data during tissue classification (Lew et al. 2013). In the BEM approach, the fontanel is incorporated into the skull shell by assigning it a thinner thickness in the corresponding locations (Roche-Labarbe et al. 2008).

In our work using real data, we determined if the fontanel represented a preferable path for electrical brain activity propagation towards the scalp surface in neonates. We found no significant difference in the EEG amplitude decay across the entire scalp surface including the midline. This may be explained by the equivalently high electrical conductivity of all tissue in the infant head. That is, no privileged pathways exist for neuronal electrical activity to travel outwards through the

fontanel. The erroneous assumptions regarding the unique role of the fontanel in the cortical signal spread stem from ignorance regarding the high conductivity of the infant skull. Our findings agree with studies showing that the fontanel structure does not significantly influence the source localisation accuracy accounted for in the head model (Roche-Labarbe et al. 2008; Despotovic et al. 2013).

6.6. Dense electrode arrays improve spatial resolution

Previous studies showed that increasing the number of recording electrodes in adults improves the spatial accuracy of EEG (Lantz et al. 2003; Yamazaki et al. 2013; Hassan et al. 2014; Welch et al. 2014). In our work, we showed that, due to the high conductivity of the neonatal skull compared to an adult skull, electrical neuronal activity spreads less, calling for the use a higher number of electrodes to monitor the infant brain. This allows for the inclusion of non-redundant information in analyses and for improvements in the spatial accuracy of disturbed functional connectivity mapping (Figure 2C).

Our simulations showed that increasing the number of EEG electrodes leads to the observation of greater cortical details. All of the tested sensor arrays, however, carried physical limitations or a 'ceiling effect'. This relates to the more substantial brain signal mixing when many cortical parcels are active rather than to an insufficient spatial sampling by the examined electrode meshes. Yet, the 'ceiling' value was still proportional to the overall number of electrodes. The drawback to the dense sensor placement includes an increasing number of spurious couplings between EEG signals due to volume conduction. A false short-range connectivity (when the same source contributes to neighbouring electrodes) can be controlled by using estimators that ignore significant zero-lag phase interactions (Stam et al. 2007; Vinck et al. 2011). But, the correction of spurious nonzero-lag synchronisation remains challenging. This problem may be alleviated by using source reconstruction methods (Schoffelen and Gross 2009; Palva et al. 2013).

Moreover, the fidelity of mathematical references, such as CSD and the global average, strictly relies on the number of electrodes. Dense electrode arrays accompany shorter inter-electrode distances, allowing for a more accurate 'local' reference for each electrode and avoiding a smoothing procedure (which distorts the original shape of brain signals) in CSD. The global average reference carries less bias due to local high-amplitude activity or artefacts when computed from a high number of EEG signals.

6.7. Montage choice matters

The choice of reference in an EEG montage may disturb the outcome of the functional connectivity analysis. This mostly relates to the robustness of different montages based on the volume conduction problem. When dealing with scalp EEG signals, no efficient means of avoiding cortical signal smearing exists. Our simulations showed that certain references may minimise such effects. When the number of electrodes remains constant, CSD and average montages become more stable in relation to volume conduction. Importantly, their fidelity significantly improves with an increase in the number of electrodes. When using 32 or more electrodes, the CSD montage showed an improved robustness to volume conduction and a higher quality towards detecting true cortical oscillations (Figure 2C). The later may be explained by the computation of a weighted local average reference for each electrode in the CSD transform. Thus, electrodes in CSD become more 'focused' on the underlying activity. This is especially important in the context of neonatal EEG given its focal nature. The performance of the CSD transform also relies on a parameter such as the smoothing factor (λ). In our work, we showed that smoothing diminishes the reliability of the connectivity analysis. This procedure acts as a spatial filter and, in fact, brings brain signals that contribute to the scalp electrodes further from their original shape. Using less than 32 electrodes, CSD and average montages showed a comparable robustness to volume conduction. Both CSD and average reference represent 'virtual' or 'mathematical' montages and can easily be computed prior to synchrony analysis despite the location of the physical reference during recording. The bias of synchrony assessment of cortical couplings increased during the testing of a monopolar montage with a common reference Cz electrode was placed at the midline (Figure 2C).

6.8. Optimising clinical recordings

This work highlights the necessity of using high-density EEG sensor arrays for quality neonatal brain monitoring and informative and spatially accurate connectivity analyses. Conventional clinical protocols typically use only a few electrodes. The most common method includes measuring EEG activity using 19 electrodes placed according to the international 10–20 system. In addition, routine clinical preference focuses on various bipolar, monopolar, and linked mastoid montages (Figure 1B). In our work, we examined all possible montages derived using 19 electrodes to define the most optimal configuration for neonatal EEG monitoring. Our results showed that, even when relatively few electrodes are used, the global average montage remains most robust to volume conduction and detects cortical signals with less distortion. The fidelity of the linked mastoids reference compared favourably with the average reference (for further details, see Figure 8

in **Study III**). In practice, however, this reference is more sensitive to movement and muscle and cardiac artefacts. Despite the moderate performance of the CSD transform using 19 electrodes, local artefacts or high amplitude fluctuations do not smear over wider areas of the scalp surface, representing more important considerations for clinical circumstances. The monopolar montage demonstrated the poorest results. Thus, the primary message is that using high-density electrode arrays in combination with a CSD montage may significantly improve the quality of clinical EEG monitoring among neonates.

6.9. Montage fidelity robust to cortical folding

We tested the fidelity of the different montages using both relatively smooth brain surfaces obtained from real anatomical MRIs and highly gyrated adult brain surfaces rescaled to a neonatal size. Importantly, in both cases the relationship between the montage fidelities remained consistent and a higher number of electrodes yielded a better spatial accuracy. In the gyrated model, the number of resolvable cortical signals from brain areas visible to EEG electrodes was less compared to those visible in the smooth model (see Figure 7 in **Study III**). This effect is quite expected since in the gyrated cortex a portion of sources deep in the sulcus carry weaker signals. Another factor includes the broader variety of dipole orientations that may lead to a signal cancellation in some cases when sources within the same parcel move in opposite directions. The gyrated model was also associated with a higher level of smearing. This may be explained by the fact that sources in the sulcus spread to a wider area on the scalp surface. Thus, the relationship between the montages in the smoothed and gyrated models we tested remained identical. The only difference between the models was in the absolute values for the different fidelity estimators (see **Study III** for more details). This finding suggests that the performance of each montage remains constant in the dynamic cortical folding processes taking place in the developing neonatal brain. Consequently, our principal results do not depend on the continuous cortical source configuration changes that take place during early brain development.

7. CONCLUSIONS

Changes in neonatal EEGs during early development reflect structural modifications, neuronal network formation, and developmental changes in inhibitory synaptic mechanisms occurring in the brain. Analysis and interpretation of such changes should be completed through the prism of these on-going processes. Furthermore, direct application of mathematical methods developed for adults without adaptation to the specific features of the neonatal EEG may yield misleading results. Conventional methods of recording infant EEGs in clinical routines may provide insufficient information since the widely used electrode arrays are heavily undersampled.

In this work, we proposed an algorithm for functional connectivity analysis of preterm infant EEG at two different temporal levels. The performance of the algorithm was tested on real EEG data from healthy infants and from infants with brain lesions. Our results show that functional connectivity at the event level may be affected by anatomical pathway disruptions. These disturbances are frequency and spatially selective, and may be revealed by analysing non-invasive EEG recordings.

Using mathematical head models and clinical EEG data, we empirically estimated the conductivity of the neonatal scalp and studied its influence on the spread of the brain's electrical signals. We concluded that its value falls in the range of 0.06 to 0.2 S/m, much higher compared to that in adults. The more conductive infant skull results the focal propagation of the brain's electrical activity from the cortex towards the scalp.

In this work, we also evaluated the fidelity of the commonly used EEG montages. We found that the choice of reference highly impacts the output of the functional connectivity analysis performed on EEG signals. The best performance was demonstrated by the high-density sensor arrays found in the CSD montage.

In this work, we put special emphasis on the practical implications of our findings in the clinical setting. In **Study I,** we optimised the proposed algorithm for neonatal EEG analysis in terms of computational efficiency and designed it to require minimal contributions from the user when accessed online. In turn, in **Study III,** we separately tested the montages limiting them to only the 19 electrodes commonly used in clinical recordings.

Acknowledgements

This thesis work was carried out at the Neuroscience Center and Department of Bioscience, Faculty of Biological and Environmental Sciences, University of Helsinki. The financial support of this work was provided by Centre for International Mobility (CIMO), Sigrid Jusélius Foundation and Finnish Cultural Foundation.

I would like to express my deepest gratitude to my supervisor Docent Sampsa Vanhatalo. It was a great opportunity and a huge pleasure to work with Sampsa during these years. I find extreme value in his attitude towards research, family and life in general. Due to his enthusiasm, his energy, his perfect grasp of the field and his deep understanding of its needs, I never had any problems with motivation. I am also grateful to my other supervisor Docent Matias Palva. His extensive experience and knowledge in the field not only made my work more interesting but also allowed me to always be learning something new. I am thankful to both my supervisors for their support, guidance and advice. It was a huge privilege and a great experience to have them both supervising my work.

I would like to thank Docent Ari Pääkkönen for kindly accepting the invitation to be an opponent at the public defense of my Dissertation.

I wish to thank the pre-examiners of my Dissertation Professor Ingmar Rosén and Assistant Professor Lauri Parkkonen for their time spent on reviewing this work and their useful comments on it.

I desire to acknowledge the members of the thesis advisory board Professor Ari Koskelainen and Dr. Alexander Zhigalov for their helpful advice and recommendations at our meetings during these years.

I want to thank Professor Juha Voipio for being my custos and for his help during these years and with the organizing of the public defense of the Dissertation.

It is hard to express with words the extent of my gratitude to Dr. Katri Wegelius, coordinator of the Brain and Mind program, for her help with numerous issues work related or not as well as for her friendly and kind relationship.

My warmest gratitude to my office mates: Muriel Lobier, Hugo Eyharabide and Felix Siebenhühner. Thank you for the cozy working environment, interesting discussions and readiness to help with any question. I want to thank Dr. Satu Palva for her friendly attitude. Huge thanks to Jonni Hirvonen, Sheng Wang, Shrikanth Kulashekhar, Hanna Julku, Santeri Rouhinen, Pantelis Lioumis, Isabel Morales Munoz, Simo Monto, Guillermo Arbilla Sampol, Jaana Simola, Sami

Karadeniz, Tom Campbell and all other past and present members of the lab for a great time together in the office and outside of it, a nice and supportive atmosphere.

I would like to thank Professor Kai Kaila who played an important role in my decision to test myself in the field of Neuroscience. I am also very grateful to him for providing me with a place and facilities at the beginning of my research work in Finland. It was also a big pleasure to meet Martin Puskarjov, Eva Ruusuvuori, Stanislav Khirug and other people during that period of my life.

I would like to mention and thank Professor Vyacheslav Shulgin who was my first scientific advisor. The knowledge and experience that I obtained during the time spent in his group were extremely useful and helpful in my further research work. In this context I would like to address my gratitude also to Leonid Krasnov, Konstantin Nasedkin and Vyacheslav Fedotenko.

I want to thank my darling wife Marina and my daughter Alexandra-Sofia who are the real meaning of life to me for their love, support, care and encouragement.

Finally, I want to express my gratitude to my parents Volodymyr and Olena and to my dear grandmother Valentina for their love, support and believing in me at all times. Special thanks to my brother Maksym who is always at my side. Я вам щиро вдячний за все, що ви для мене зробили, за вашу підтримку та любов.

Reference List

Adelsberger H, Garaschuk O, Konnerth A. 2005. Cortical calcium waves in resting newborn mice. Nat Neurosci. 8:988–990.

Akalin-Acar Z, Gençer NG. 2004. An advanced boundary element method (BEM) implementation for the forward problem of electromagnetic source imaging. Phys Med Biol. 49:5011–5028.

Akhtari M, Bryant HC, Mamelak AN, Flynn ER, Heller L, Shih JJ, Mandelkern M, Matlachov A, Ranken DM, Best ED, DiMauro MA, Lee RR, Sutherling WW. 2002. Conductivities of three-layer live human skull. Brain Topogr. 14:151–167.

André M, Lamblin MD, d'Allest AM, Curzi-Dascalova L, Moussalli-Salefranque F, The SN, Vecchierini-Blineau MF, Wallois F, Walls-Esquivel E, Plouin P. 2010. Electroencephalography in premature and full-term infants. Developmental features and glossary. Clin Neurophysiol. 40:59–124.

Aydore S, Pantazis D, Leahy RM. 2013. A note on the phase locking value and its properties. Neuroimage. 74:231–244.

Baillet S, Mosher JC, Leahy RM. 2001. Electromagnetic brain mapping. Signal Processing Magazine, IEEE. 18:14–30.

Ben-Ari Y. 2001. Developing networks play a similar melody. Trends Neurosci. 24:353–360.

Bender VA, Bender KJ, Brasier DJ, Feldman DE. 2006. Two coincidence detectors for spike timing-dependent plasticity in somatosensory cortex. J Neurosci. 26:4166–4177.

Blankenship AG, Feller MB. 2010. Mechanisms underlying spontaneous patterned activity in developing neural circuits. Nat Rev Neurosci. 11:18–29.

Bressler SL, Menon V. 2010. Large-scale brain networks in cognition: emerging methods and principles. Trends Cogn Sci. 14:277–290.

Brookes MJ, Woolrich MW, Barnes GR. 2012. Measuring functional connectivity in MEG: a multivariate approach insensitive to linear source leakage. Neuroimage. 63:910–920.

Bruns A. 2004. Fourier-, Hilbert- and wavelet-based signal analysis: are they really different approaches? J Neurosci Methods. 137:321–332.

Bruns A, Eckhorn R, Jokeit H, Ebner A. 2000. Amplitude envelope correlation detects coupling among incoherent brain signals. Neuroreport. 11:1509–1514.

Buchner H, Knoll G, Fuchs M, Rienäcker A, Beckmann R, Wagner M, Silny J, Pesch J. 1997. Inverse localization of electric dipole current sources in finite element models of the human head. Electroencephalogr Clin Neurophysiol. 102:267–278.

Buzsaki G, Anastassiou CA, Koch C. 2012. The origin of extracellular fields and currents-EEG, ECoG, LFP and spikes. Nat Rev Neurosci. 13:407–420.

Buzsaki G, Draguhn A. 2004. Neuronal oscillations in cortical networks. Science. 304:1926–1929.

Canolty RT, Knight RT. 2010. The functional role of cross-frequency coupling. Trends Cogn Sci. 14:506–515.

Cheng AHD, Cheng DT. 2005. Heritage and early history of the boundary element method. Engineering Analysis with Boundary Elements. 29:268–302.

Cherniak C, Mokhtarzada Z, Rodriguez-Esteban R, Changizi K. 2004. Global optimization of cerebral cortex layout. Proc Natl Acad Sci U S A. 101:1081–1086.

Chklovskii DB, Schikorski T, Stevens CF. 2002. Wiring optimization in cortical circuits. Neuron. 34:341–347.

Cho JH, Vorwerk J, Wolters CH, Knösche TR. 2015. Influence of the head model on EEG and MEG source connectivity analyses. Neuroimage. 110:60–77.

Clough RW. 2004. Early history of the finite element method from the view point of a pioneer. International Journal for Numerical Methods in Engineering. 60:283–287.

Colonnese MT, Khazipov R. 2012. Spontaneous activity in developing sensory circuits: Implications for resting state fMRI. Neuroimage. 62:2212–2221.

Dekaban AS. 1978. Changes in brain weights during the span of human life: relation of brain weights to body heights and body weights. Ann Neurol. 4:345–356.

Despotovic I, Cherian PJ, De VM, Hallez H, Deburchgraeve W, Govaert P, Lequin M, Visser GH, Swarte RM, Vansteenkiste E, Van HS, Philips W. 2013. Relationship of EEG sources of neonatal seizures to acute perinatal brain lesions seen on MRI: a pilot study. Hum Brain Mapp. 34:2402–2417.

Doria V, Beckmann CF, Arichi T, Merchant N, Groppo M, Turkheimer FE, Counsell SJ, Murgasova M, Aljabar P, Nunes RG, Larkman DJ, Rees G, Edwards AD. 2010. Emergence of resting state networks in the preterm human brain. Proc Natl Acad Sci U S A. 107:20015–20020.

Dubois J, Benders M, Borradori-Tolsa C, Cachia A, Lazeyras F, Ha-Vinh LR, Sizonenko SV, Warfield SK, Mangin JF, Huppi PS. 2008a. Primary cortical folding in the human newborn: an early marker of later functional development. Brain. 131:2028–2041.

Dubois J, Benders M, Cachia A, Lazeyras F, Ha-Vinh LR, Sizonenko SV, Borradori-Tolsa C, Mangin JF, Huppi PS. 2008b. Mapping the early cortical folding process in the preterm newborn brain. Cereb Cortex. 18:1444–1454.

Dubois J, Dehaene-Lambertz G, Kulikova S, Poupon C, Huppi PS, Hertz-Pannier L. 2014. The early development of brain white matter: a review of imaging studies in fetuses, newborns and infants. Neuroscience. 276:48–71.

Dudink J, Kerr JL, Paterson K, Counsell SJ. 2008. Connecting the developing preterm brain. Early Hum Dev. 84:777–782.

Dupont E, Hanganu IL, Kilb W, Hirsch S, Luhmann HJ. 2006. Rapid developmental switch in the mechanisms driving early cortical columnar networks. Nature. 439:79–83.

Dzhala VI, Talos DM, Sdrulla DA, Brumback AC, Mathews GC, Benke TA, Delpire E, Jensen FE, Staley KJ. 2005. NKCC1 transporter facilitates seizures in the developing brain. Nat Med. 11:1205–1213.

Engel AK, Gerloff C, Hilgetag CC, Nolte G. 2013. Intrinsic coupling modes: multiscale interactions in ongoing brain activity. Neuron. 80:867–886.

Erasmie U, Ringertz H. 1976. Normal width of cranial sutures in the neonate and infant. An objective method of assessment. Acta Radiol Diagn (Stockh). 17:565–572.

Ernst LM. 2011. Bone. In: Ernst LM, Ruchelli ED, Huff DS, editors. Color Atlas of Fetal and Neonatal Histology. New York: Springer-Verlag. p 323–336.

Espinosa JS, Stryker MP. 2012. Development and plasticity of the primary visual cortex. Neuron. 75:230–249.

Essl M, Rappelsberger P. 1998. EEG coherence and reference signals: experimental results and mathematical explanations. Med Biol Eng Comput. 36:399–406.

Feller MB, Scanziani M. 2005. A precritical period for plasticity in visual cortex. Curr Opin Neurobiol. 15:94–100.

Fischl B, Liu A, Dale AM. 2001. Automated manifold surgery: Constructing geometrically accurate and topologically correct models of the human cerebral cortex. Ieee Transactions on Medical Imaging. 20:70–80.

Freunberger R, Fellinger R, Sauseng P, Gruber W, Klimesch W. 2009. Dissociation between phase-locked and nonphase-locked alpha oscillations in a working memory task. Hum Brain Mapp. 30:3417–3425.

Fries P. 2005. A mechanism for cognitive dynamics: neuronal communication through neuronal coherence. Trends Cogn Sci. 9:474–480.

Frijns JH, de Snoo SL, Schoonhoven R. 2000. Improving the accuracy of the boundary element method by the use of second-order interpolation functions. IEEE Trans Biomed Eng. 47:1336–1346.

Friston KJ, Harrison L, Penny W. 2003. Dynamic causal modelling. Neuroimage. 19:1273–1302.

Fuchs M, Wagner M, Kastner J. 2001. Boundary element method volume conductor models for EEG source reconstruction. Clin Neurophysiol. 112:1400–1407.

Gençer NG, Acar CE. 2004. Sensitivity of EEG and MEG measurements to tissue conductivity. Phys Med Biol. 49:701–717.

Gençer NG, Tanzer IO. 1999. Forward problem solution of electromagnetic source imaging using a new BEM formulation with high-order elements. Phys Med Biol. 44:2275–2287.

Glickfeld LL, Roberts JD, Somogyi P, Scanziani M. 2009. Interneurons hyperpolarize pyramidal cells along their entire somatodendritic axis. Nat Neurosci. 12:21–23.

Goldman D. 1950. The clinical use of the "average" reference electrode in monopolar recording. Electroencephalogr Clin Neurophysiol. 2:209–212.

Gonzalez JJ, Manas S, De VL, Mendez LD, Lopez S, Garrido JM, Pereda E. 2011. Assessment of electroencephalographic functional connectivity in term and preterm neonates. Clin Neurophysiol. 122:696–702.

Gramfort A, Papadopoulo T, Olivi E, Clerc M. 2010. OpenMEEG: opensource software for quasistatic bioelectromagnetics. Biomed Eng Online. 9:45.

Granger CWJ. 1969. Investigating causal relations by econometric models and cross-spectral methods. Econometrica. 37:424–438.

Grech R, Cassar T, Muscat J, Camilleri KP, Fabri SG, Zervakis M, Xanthopoulos P, Sakkalis V, Vanrumste B. 2008. Review on solving the inverse problem in EEG source analysis. J Neuroeng Rehabil. 5:25.

Grieve PG, Emerson RG, Fifer WP, Isler JR, Stark RI. 2003. Spatial correlation of the infant and adult electroencephalogram. Clin Neurophysiol. 114:1594–1608.

Grieve PG, Emerson RG, Isler JR, Stark RI. 2004. Quantitative analysis of spatial sampling error in the infant and adult electroencephalogram. Neuroimage. 21:1260–1274.

Grieve PG, Isler JR, Izraelit A, Peterson BS, Fifer WP, Myers MM, Stark RI. 2008. EEG functional connectivity in term age extremely low birth weight infants. Clin Neurophysiol. 119:2712–2720.

Grossmann A, Kronland-Martinet R, Morlet J. 1989. Reading and understanding continuous wavelets transforms. In: Combes JM, Grossmann A, Tchamitchian P, editors. Wavelets, Time-Frequency Methods and Phase Space. New York: Springer-Verlag. p 2–20.

Gutierrez D, Nehorai A, Muravchik CH. 2004. Estimating brain conductivities and dipole source signals with EEG arrays. Ieee Transactions on Biomedical Engineering. 51:2113–2122.

Hagemann D, Naumann E, Thayer JF. 2001. The quest for the EEG reference revisited: a glance from brain asymmetry research. Psychophysiology. 38:847–857.

Hahn JS, Tharp BR. 1990. Winner of the Brazier Award. The dysmature EEG pattern in infants with bronchopulmonary dysplasia and its prognostic implications. Electroencephalogr Clin Neurophysiol. 76:106–113.

Hallez H, Vanrumste B, Grech R, Muscat J, De CW, Vergult A, D'Asseler Y, Camilleri KP, Fabri SG, Van HS, Lemahieu I. 2007. Review on solving the forward problem in EEG source analysis. J Neuroeng Rehabil. 4:46.

Hämäläinen JA, Ortiz-Mantilla S, Benasich AA. 2011. Source localization of event-related potentials to pitch change mapped onto age-appropriate MRIs at 6 months of age. Neuroimage. 54:1910–1918.

Hämäläinen MS, Sarvas J. 1989. Realistic conductivity geometry model of the human head for interpretation of neuromagnetic data. IEEE Trans Biomed Eng. 36:165–171.

Hanganu-Opatz IL. 2010. Between molecules and experience: role of early patterns of coordinated activity for the development of cortical maps and sensory abilities. Brain Res Rev. 64:160–176.

Hassan M, Dufor O, Merlet I, Berrou C, Wendling F. 2014. EEG source connectivity analysis: from dense array recordings to brain networks. PLoS One. 9:e105041.

Haueisen J, Ramon C, Czapski P, Eiselt M. 1995. On the influence of volume currents and extended sources on neuromagnetic fields: a simulation study. Ann Biomed Eng. 23:728–739.

Haufe S, Nikulin VV, Muller KR, Nolte G. 2013. A critical assessment of connectivity measures for EEG data: a simulation study. Neuroimage. 64:120–133.

He BJ, Zempel JM, Snyder AZ, Raichle ME. 2010. The temporal structures and functional significance of scale-free brain activity. Neuron. 66:353–369.

Hebb DO. 1949. The Organization of Behavior: A Neuropsychological Theory. New York: John Wiley and Sons.

Hipp JF, Hawellek DJ, Corbetta M, Siegel M, Engel AK. 2012. Large-scale cortical correlation structure of spontaneous oscillatory activity. Nat Neurosci. 15:884–890.

Hjorth B. 1975. An on-line transformation of EEG scalp potentials into orthogonal source derivations. Electroencephalogr Clin Neurophysiol. 39:526–530.

Hsiao GC. 2006. Boundary element methods - An overview. Applied Numerical Mathematics. 56:1356–1369.

Hughes JG, DAVIS BC, BRENNAN ML. 1951. Electroencephalography of the newborn infant. VI. Studies on premature infants. Pediatrics. 7:707–712.

Hüppi PS, Warfield S, Kikinis R, Barnes PD, Zientara GP, Jolesz FA, Tsuji MK, Volpe JJ. 1998. Quantitative magnetic resonance imaging of brain development in premature and mature newborns. Ann Neurol. 43:224–235.

Irimia A, Goh SY, Torgerson CM, Chambers MC, Kikinis R, Van Horn JD. 2013. Forward and inverse electroencephalographic modeling in health and in acute traumatic brain injury. Clin Neurophysiol. 124:2129–2145.

Jafarian N, Kazemi K, Moghaddam HA, Grebe R, Fournier M, Helfroush MS, Gondry-Jouet C, Wallois F. 2014. Automatic segmentation of newborns' skull and fontanel from CT data using model-based variational level set. Signal Image and Video Processing. 8:377–387.

Jasper HH. 1958. Report of the Committee on Methods of Clinical Examination in Electroencephalography. Electroenceph Clin Neurophysiol. 10:370–375.

Jennekens W, Dankers F, Blijham P, Cluitmans P, van PC, Andriessen P. 2013. EEG source localization in full-term newborns with hypoxic-ischemia. Conf Proc IEEE Eng Med Biol Soc. 2013:3291–3294.

Jervis BW, Nichols MJ, Johnson TE, Allen E, Hudson NR. 1983. A fundamental investigation of the composition of auditory evoked potentials. IEEE Trans Biomed Eng. 30:43–50.

Joris PX, Smith PH, Yin TC. 1998. Coincidence detection in the auditory system: 50 years after Jeffress. Neuron. 21:1235–1238.

Judas M, Rados M, Jovanov-Milosevic N, Hrabac P, Stern-Padovan R, Kostovic I. 2005. Structural, immunocytochemical, and mr imaging properties of periventricular crossroads of growing cortical pathways in preterm infants. AJNR Am J Neuroradiol. 26:2671–2684.

Kapellou O, Counsell SJ, Kennea N, Dyet L, Saeed N, Stark J, Maalouf E, Duggan P, Ajayi-Obe M, Hajnal J, Allsop JM, Boardman J, Rutherford MA, Cowan F, Edwards AD. 2006. Abnormal cortical development after premature birth shown by altered allometric scaling of brain growth. PLoS Med. 3:e265.

Katz LC. 1993. Coordinate activity in retinal and cortical development. Curr Opin Neurobiol. 3:93–99.

Katz LC, Shatz CJ. 1996. Synaptic activity and the construction of cortical circuits. Science. 274:1133–1138.

Kayser J, Tenke CE. 2006a. Principal components analysis of Laplacian waveforms as a generic method for identifying ERP generator patterns: I. Evaluation with auditory oddball tasks. Clin Neurophysiol. 117:348–368.

Kayser J, Tenke CE. 2006b. Principal components analysis of Laplacian waveforms as a generic method for identifying ERP generator patterns: II. Adequacy of low-density estimates. Clin Neurophysiol. 117:369–380.

Khazipov R, Luhmann HJ. 2006. Early patterns of electrical activity in the developing cerebral cortex of humans and rodents. Trends Neurosci. 29:414–418.

Kilb W, Kirischuk S, Luhmann HJ. 2011. Electrical activity patterns and the functional maturation of the neocortex. Eur J Neurosci. 34:1677–1686.

Klyachko VA, Stevens CF. 2003. Connectivity optimization and the positioning of cortical areas. Proc Natl Acad Sci U S A. 100:7937–7941.

Knickmeyer RC, Gouttard S, Kang C, Evans D, Wilber K, Smith JK, Hamer RM, Lin W, Gerig G, Gilmore JH. 2008. A structural MRI study of human brain development from birth to 2 years. J Neurosci. 28:12176–12182.

Kostovic I, Jovanov-Milosevic N. 2006. The development of cerebral connections during the first 20–45 weeks' gestation. Semin Fetal Neonatal Med. 11:415–422.

Kostovic I, Judas M. 2006. Prolonged coexistence of transient and permanent circuitry elements in the developing cerebral cortex of fetuses and preterm infants. Dev Med Child Neurol. 48:388–393.

Kostovic I, Judas M. 2010. The development of the subplate and thalamocortical connections in the human foetal brain. Acta Paediatr. 99:1119–1127.

Kostovic I, Rakic P. 1990. Developmental history of the transient subplate zone in the visual and somatosensory cortex of the macaque monkey and human brain. J Comp Neurol. 297:441–470.

Kronland-Martinet R, Morlet J, Grossmann A. 1987. Analysis of sound patterns through wavelet transforms. Int J Patt Recogn Art Intell. 1:273–302.

Kuks JB, Vos JE, O'Brien MJ. 1988. EEG coherence functions for normal newborns in relation to their sleep state. Electroencephalogr Clin Neurophysiol. 69:295–302.

Kybic J, Clerc M, Abboud T, Faugeras O, Keriven R, Papadopoulo T. 2005. A common formalism for the integral formulations of the forward EEG problem. IEEE Trans Med Imaging. 24:12–28.

Lachaux JP, Rodriguez E, Martinerie J, Varela FJ. 1999. Measuring phase synchrony in brain signals. Hum Brain Mapp. 8:194–208.

Lachaux JP, Rodriguez E, Van Quyen ML, Lutz A, Martinerie J, Varela FJ. 2000. Studying single-trials of phase synchronous activity in the brain. International Journal of Bifurcation and Chaos. 10:2429–2439.

Lai Y, van DW, Ding L, Hecox KE, Towle VL, Frim DM, He B. 2005. Estimation of in vivo human brain-to-skull conductivity ratio from simultaneous extra- and intra-cranial electrical potential recordings. Clin Neurophysiol. 116:456–465.

Lakatos P, Karmos G, Mehta AD, Ulbert I, Schroeder CE. 2008. Entrainment of neuronal oscillations as a mechanism of attentional selection. Science. 320:110–113.

Lamblin MD, André M, Challamel MJ, Curzi-Dascalova L, d'Allest AM, De GE, Moussalli-Salefranque F, Navelet Y, Plouin P, Radvanyi-Bouvet MF, Samson-Dollfus D, Vecchierini-Blineau MF. 1999. Electroencephalography of the premature and term newborn. Maturational aspects and glossary. Neurophysiol Clin. 29:123–219.

Lantz G, Grave de PR, Spinelli L, Seeck M, Michel CM. 2003. Epileptic source localization with high density EEG: how many electrodes are needed? Clin Neurophysiol. 114:63–69.

Le Van Quyen M, Foucher J, Lachaux J, Rodriguez E, Lutz A, Martinerie J, Varela FJ. 2001. Comparison of Hilbert transform and wavelet methods for the analysis of neuronal synchrony. J Neurosci Methods. 111:83–98.

Lew S, Sliva DD, Choe MS, Grant PE, Okada Y, Wolters CH, Hamalainen MS. 2013. Effects of sutures and fontanels on MEG and EEG source analysis in a realistic infant head model. Neuroimage. 76:282–293.

Lin W, Zhu Q, Gao W, Chen Y, Toh CH, Styner M, Gerig G, Smith JK, Biswal B, Gilmore JH. 2008. Functional connectivity MR imaging reveals cortical functional connectivity in the developing brain. AJNR Am J Neuroradiol. 29:1883–1889.

Lobier M, Siebenhuhner F, Palva S, Palva JM. 2014. Phase transfer entropy: a novel phase-based measure for directed connectivity in networks coupled by oscillatory interactions. Neuroimage. 85 Pt 2:853–872.

Loomis AL, Newton HE, Garret H. 1938. Electrical potentials of the human brain. J Exp Psychol. 29:249–279.

Lopes da Silva F. 2004. Functional localization of brain sources using EEG and/or MEG data: volume conductor and source models. Magn Reson Imaging. 22:1533–1538.

Mai H, SCHUTZ E, MULLER HW. 1951. The electroencephalogram of the premature infant. Z Kinderheilkd. 69:251–261.

Marcano-Reik AJ, Prasad T, Weiner JA, Blumberg MS. 2010. An abrupt developmental shift in callosal modulation of sleep-related spindle bursts coincides with the emergence of excitatory-inhibitory balance and a reduction of somatosensory cortical plasticity. Behav Neurosci. 124:600–611.

McConnell SK, Ghosh A, Shatz CJ. 1989. Subplate neurons pioneer the first axon pathway from the cerebral cortex. Science. 245:978–982.

Meyerson BA. 1968. Ontogeny of interhemispheric functions. An electrophysiological study in pre- and postnatal sheep. Acta Physiol Scand Suppl. 312:1–111.

Milde T, Putsche P, Schwab K, Wacker M, Eiselt M, Witte H. 2011. Dynamics of directed interactions between brain regions during interburst-burst EEG patterns in quiet sleep of full-term neonates. Neurosci Lett. 488:148–153.

Mima T, Hallett M. 1999. Electroencephalographic analysis of cortico-muscular coherence: reference effect, volume conduction and generator mechanism. Clin Neurophysiol. 110:1892–1899.

Molliver ME, Kostovic I, van der Loos H. 1973. The development of synapses in cerebral cortex of the human fetus. Brain Res. 50:403–407.

Monto S. 2012. Nested synchrony-a novel cross-scale interaction among neuronal oscillations. Front Physiol. 3:384.

Mormann F, Lehnertz K, David P, Elger CE. 2000. Mean phase coherence as a measure for phase synchronization and its application to the EEG of epilepsy patients. Physica D. 144:358–369.

Mosher JC, Leahy RM, Lewis PS. 1999. EEG and MEG: forward solutions for inverse methods. IEEE Trans Biomed Eng. 46:245–259.

Mountcastle VB. 1997. The columnar organization of the neocortex. Brain. 120 (Pt 4):701–722.

Mrzljak L, Uylings HB, Kostovic I, van Eden CG. 1988. Prenatal development of neurons in the human prefrontal cortex: I. A qualitative Golgi study. J Comp Neurol. 271:355–386.

Musacchia G, Choudhury NA, Ortiz-Mantilla S, Realpe-Bonilla T, Roesler CP, Benasich AA. 2013. Oscillatory support for rapid frequency change processing in infants. Neuropsychologia. 51:2812–2824.

Musha T, Okamoto Y. 1999. Forward and inverse problems of EEG dipole localization. Crit Rev Biomed Eng. 27:189–239.

Nolte G, Bai O, Wheaton L, Mari Z, Vorbach S, Hallett M. 2004. Identifying true brain interaction from EEG data using the imaginary part of coherency. Clin Neurophysiol. 115:2292–2307.

Nunez PL, Silberstein RB. 2000. On the relationship of synaptic activity to macroscopic measurements: does co-registration of EEG with fMRI make sense? Brain Topogr. 13:79–96.

Nunez PL, Silberstein RB, Shi Z, Carpenter MR, Srinivasan R, Tucker DM, Doran SM, Cadusch PJ, Wijesinghe RS. 1999. EEG coherency II: experimental comparisons of multiple measures. Clin Neurophysiol. 110:469–486.

Nunez PL, Srinivasan R. 2006. Electric Fields of the Brain: The Neurophysics of EEG. New York: Oxford University Press.

Nunez PL, Srinivasan R, Westdorp AF, Wijesinghe RS, Tucker DM, Silberstein RB, Cadusch PJ. 1997. EEG coherency. I: Statistics, reference electrode, volume conduction, Laplacians, cortical imaging, and interpretation at multiple scales. Electroencephalogr Clin Neurophysiol. 103:499–515.

Odabaee M, Freeman WJ, Colditz PB, Ramon C, Vanhatalo S. 2013. Spatial patterning of the neonatal EEG suggests a need for a high number of electrodes. Neuroimage. 68:229–235.

Offner FF. 1950. The EEG as potential mapping: the value of the average monopolar reference. Electroencephalogr Clin Neurophysiol. 2:213–214.

Omidvarnia A, Azemi G, Boashash B, O'Toole JM, Colditz PB, Vanhatalo S. 2014a. Measuring time-varying information flow in scalp EEG signals: orthogonalized partial directed coherence. IEEE Trans Biomed Eng. 61:680–693.

Omidvarnia A, Fransson P, Metsaranta M, Vanhatalo S. 2014b. Functional bimodality in the brain networks of preterm and term human newborns. Cereb Cortex. 24:2657–2668.

Oostendorp TF, Delbeke J, Stegeman DF. 2000. The conductivity of the human skull: results of in vivo and in vitro measurements. IEEE Trans Biomed Eng. 47:1487–1492.

Ortiz-Mantilla S, Hämäläinen JA, Benasich AA. 2012. Time course of ERP generators to syllables in infants: a source localization study using age-appropriate brain templates. Neuroimage. 59:3275–3287.

Pallas SL. 2001. Intrinsic and extrinsic factors that shape neocortical specification. Trends Neurosci. 24:417–423.

Palmu K, Kirjavainen T, Stjerna S, Salokivi T, Vanhatalo S. 2013. Sleep wake cycling in early preterm infants: Comparison of polysomnographic recordings with a novel EEG-based index. Clinical Neurophysiology. 124:1807–1814.

Palmu K, Stevenson N, Wikström S, Hellström-Westas L, Vanhatalo S, Palva JM. 2010a. Optimization of an NLEO-based algorithm for automated detection of spontaneous activity transients in early preterm EEG. Physiol Meas. 31:85–93.

Palmu K, Wikström S, Hippeläinen E, Boylan G, Hellström-Westas L, Vanhatalo S. 2010b. Detection of 'EEG bursts' in the early preterm EEG: visual vs. automated detection. Clin Neurophysiol. 121:1015–1022.

Palva JM, Monto S, Kulashekhar S, Palva S. 2010. Neuronal synchrony reveals working memory networks and predicts individual memory capacity. Proc Natl Acad Sci U S A. 107:7580–7585.

Palva JM, Palva S. 2011. Roles of multiscale brain activity fluctuations in shaping the variability and dynamics of psychophysical performance. Prog Brain Res. 193:335–350.

Palva JM, Palva S, Kaila K. 2005. Phase synchrony among neuronal oscillations in the human cortex. J Neurosci. 25:3962–3972.

Palva JM, Zhigalov A, Hirvonen J, Korhonen O, Linkenkaer-Hansen K, Palva S. 2013. Neuronal long-range temporal correlations and avalanche dynamics are correlated with behavioral scaling laws. Proc Natl Acad Sci U S A. 110:3585–3590.

Palva S, Palva JM. 2012. Discovering oscillatory interaction networks with M/EEG: challenges and breakthroughs. Trends Cogn Sci. 16:219–230.

Pascual-Marqui RD, Lehmann D. 1993. Topographic maps, source localization inference, and the reference electrode: comments on a paper by Desmedt et al. Electroencephalogr Clin Neurophysiol. 88:532–536.

Paul K, Krajca V, Roth Z, Melichar J, Petranek S. 2003. Comparison of quantitative EEG characteristics of quiet and active sleep in newborns. Sleep Med. 4:543–552.

Penn AA, Shatz CJ. 1999. Brain waves and brain wiring: the role of endogenous and sensory-driven neural activity in development. Pediatr Res. 45:447–458.

Penny WD, Litvak V, Fuentemilla L, Duzel E, Friston K. 2009. Dynamic Causal Models for phase coupling. J Neurosci Methods. 183:19–30.

Prastawa M, Gilmore JH, Lin W, Gerig G. 2005. Automatic segmentation of MR images of the developing newborn brain. Med Image Anal. 9:457–466.

Price DJ, Kennedy H, Dehay C, Zhou L, Mercier M, Jossin Y, Goffinet AM, Tissir F, Blakey D, Molnar Z. 2006. The development of cortical connections. Eur J Neurosci. 23:910–920.

Ramakers GJ. 2005. Neuronal network formation in human cerebral cortex. Prog Brain Res. 147:1–14.

Ramon C, Haueisen J, Schimpf PH. 2006a. Influence of head models on neuromagnetic fields and inverse source localizations. Biomed Eng Online. 5:55.

Ramon C, Schimpf P, Haueisen J, Holmes M, Ishimaru A. 2004. Role of soft bone, CSF and gray matter in EEG simulations. Brain Topogr. 16:245–248.

Ramon C, Schimpf PH, Haueisen J. 2006b. Influence of head models on EEG simulations and inverse source localizations. Biomed Eng Online. 5:10.

Räsänen O, Metsäranta M, Vanhatalo S. 2013. Development of a novel robust measure for interhemispheric synchrony in the neonatal EEG: activation synchrony index (ASI). Neuroimage. 69:256–266.

Reynolds GD, Richards JE. 2009. Cortical source localization of infant cognition. Dev Neuropsychol. 34:312–329.

Roche-Labarbe N, Aarabi A, Kongolo G, Gondry-Jouet C, Dumpelmann M, Grebe R, Wallois F. 2008. High-resolution electroencephalography and source localization in neonates. Hum Brain Mapp. 29:167–176.

Savitzky A, Golay MJE. 1964. Smoothing and differentiation of data by simplified least squares procedures. Analytical Chemistry. 36:1627–1639.

Scher MS. 2005. Electroencephalography of the Newborn: Normal and Abnormal Features. In: Niedermeyer E, Lopes da Silva F, editors. Electroencephalography: Basic Principles, Clinical Applications, and Related Fields. Philadelphia: Lippincott Williams & Wilkins. p 937–990.

Schoffelen JM, Gross J. 2009. Source connectivity analysis with MEG and EEG. Hum Brain Mapp. 30:1857–1865.

Schreiber T. 2000. Measuring information transfer. Phys Rev Lett. 85:461–464.

Segonne F, Pacheco J, Fischl B. 2007. Geometrically accurate topology-correction of cortical surfaces using nonseparating loops. Ieee Transactions on Medical Imaging. 26:518–529.

Selton D, André M, Hascoet JM. 2000. Normal EEG in very premature infants: reference criteria. Clin Neurophysiol. 111:2116–2124.

Shi F, Fan Y, Tang S, Gilmore JH, Lin W, Shen D. 2010. Neonatal brain image segmentation in longitudinal MRI studies. Neuroimage. 49:391–400.

Singer W. 1995. Development and plasticity of cortical processing architectures. Science. 270:758–764.

Singer W. 1999. Neuronal synchrony: a versatile code for the definition of relations? Neuron. 24:49–25.

Sipilä ST, Huttu K, Soltesz I, Voipio J, Kaila K. 2005. Depolarizing GABA acts on intrinsically bursting pyramidal neurons to drive giant depolarizing potentials in the immature hippocampus. J Neurosci. 25:5280–5289.

Sipilä ST, Kaila K. 2008. GABAergic control of CA3-driven network events in the developing hippocampus. Results Probl Cell Differ. 44:99–121.

Smith JR. 1938. The electroencephalogram during normal infancy and childhood. I. Rhythmic activities present in the neonate and their subsequent development. J Gen Psychol. 53:431–453.

Smyser CD, Inder TE, Shimony JS, Hill JE, Degnan AJ, Snyder AZ, Neil JJ. 2010. Longitudinal analysis of neural network development in preterm infants. Cerebral Cortex. 20:2852–2862.

Song J, Turovets S, Govyadinov P, Mattson C, Luu P, Smith K, Prior F, Larson-Prior L, Tucker DM. 2013. Anatomically accurate infant head models for EEG source localization. J Phys: Conf Ser. 434:1–4.

Sporns O. 2011. Networks of the brain. Cambridge, Mass: MIT Press, USA.

Stam CJ, Nolte G, Daffertshofer A. 2007. Phase lag index: assessment of functional connectivity from multi channel EEG and MEG with diminished bias from common sources. Hum Brain Mapp. 28:1178–1193.

Steriade M. 2006. Grouping of brain rhythms in corticothalamic systems. Neuroscience. 137:1087–1106.

Stjerna S, Voipio J, Metsäranta M, Kaila K, Vanhatalo S. 2012. Preterm EEG: a multimodal neurophysiological protocol. J Vis Exp. e3774.

Tallon-Baudry C, Bertrand O, Delpuech C, Permier J. 1997. Oscillatory gamma-band (30-70 Hz) activity induced by a visual search task in humans. J Neurosci. 17:722–734.

Tau GZ, Peterson BS. 2010. Normal development of brain circuits. Neuropsychopharmacology. 35:147–168.

Tenke CE, Kayser J. 2012. Generator localization by current source density (CSD): implications of volume conduction and field closure at intracranial and scalp resolutions. Clin Neurophysiol. 123:2328–2345.

Tognoli E, Kelso JA. 2009. Brain coordination dynamics: true and false faces of phase synchrony and metastability. Prog Neurobiol. 87:31–40.

Tokariev A, Videman M, Palva JM, Vanhatalo S. Brain connectivity changes between vigilance states and develops rapidly around term age in the human newborn. Unpublished Work.

Tolonen M, Palva JM, Andersson S, Vanhatalo S. 2007. Development of the spontaneous activity transients and ongoing cortical activity in human preterm babies. Neuroscience. 145:997–1006.

Tononi G, Sporns O, Edelman GM. 1994. A measure for brain complexity: relating functional segregation and integration in the nervous system. Proc Natl Acad Sci U S A. 91:5033–5037.

Towle VL, Bolanos J, Suarez D, Tan K, Grzeszczuk R, Levin DN, Cakmur R, Frank SA, Spire JP. 1993. The spatial location of EEG electrodes: locating the best-fitting sphere relative to cortical anatomy. Electroencephalogr Clin Neurophysiol. 86:1–6.

Trevelyan AJ. 2009. The direct relationship between inhibitory currents and local field potentials. J Neurosci. 29:15299–15307.

Uhlhaas PJ, Pipa G, Lima B, Melloni L, Neuenschwander S, Nikolic D, Singer W. 2009. Neural synchrony in cortical networks: history, concept and current status. Front Integr Neurosci. 3:17.

Uhlhaas PJ, Roux F, Rodriguez E, Rotarska-Jagiela A, Singer W. 2010. Neural synchrony and the development of cortical networks. Trends Cogn Sci. 14:72–80.

Vanhatalo S, Kaila K. 2006. Development of neonatal EEG activity: from phenomenology to physiology. Semin Fetal Neonatal Med. 11:471–478.

Vanhatalo S, Kaila K. 2010. Emergence of spontaneous and evoked EEG activity in the human brain. In: Lagercrantz H, Hanson MA, Ment LR, Peebles DM, editors. The Newborn Brain: Neuroscience and Clinical Applications. Cambridge: Cambridge University Press. p 229–243.

Vanhatalo S, Metsäranta M, Andersson S. 2008. High-fidelity recording of brain activity in the extremely preterm babies: feasibility study in the incubator. Clin Neurophysiol. 119:439–445.

Vanhatalo S, Palva JM. 2011. Phase brings a new phase to the exploration of the elusive neonatal EEG. Clin Neurophysiol. 122:645–647.

Vanhatalo S, Palva JM, Andersson S, Rivera C, Voipio J, Kaila K. 2005a. Slow endogenous activity transients and developmental expression of K+-Cl– cotransporter 2 in the immature human cortex. Eur J Neurosci. 22:2799–2804.

Vanhatalo S, Palva JM, Holmes MD, Miller JW, Voipio J, Kaila K. 2004. Infraslow oscillations modulate excitability and interictal epileptic activity in the human cortex during sleep. Proc Natl Acad Sci U S A. 101:5053–5057.

Vanhatalo S, Voipio J, Kaila K. 2005b. Full-band EEG (FbEEG): an emerging standard in electroencephalography. Clin Neurophysiol. 116:1–8.

Varela F, Lachaux JP, Rodriguez E, Martinerie J. 2001. The brainweb: phase synchronization and large-scale integration. Nat Rev Neurosci. 2:229–239.

Vecchierini MF, d'Allest AM, Verpillat P. 2003. EEG patterns in 10 extreme premature neonates with normal neurological outcome: qualitative and quantitative data. Brain Dev. 25:330–337.

Vinck M, Oostenveld R, van WM, Battaglia F, Pennartz CM. 2011. An improved index of phase-synchronization for electrophysiological data in the presence of volume-conduction, noise and sample-size bias. Neuroimage. 55:1548–1565.

Wallois F, Patil A, Kongolo G, Goudjil S, Grebe R. 2009. Haemodynamic changes during seizure-like activity in a neonate: a simultaneous AC EEG-SPIR and high-resolution DC EEG recording. Neurophysiol Clin. 39:217–227.

Walsh BH, Murray DM, Boylan GB. 2011. The use of conventional EEG for the assessment of hypoxic ischaemic encephalopathy in the newborn: a review. Clin Neurophysiol. 122:1284–1294.

Weisenfeld NI, Warfield SK. 2009. Automatic segmentation of newborn brain MRI. Neuroimage. 47:564–572.

Welch MG, Myers MM, Grieve PG, Isler JR, Fifer WP, Sahni R, Hofer MA, Austin J, Ludwig RJ, Stark RI. 2014. Electroencephalographic activity of preterm infants is increased by Family Nurture Intervention: a randomized controlled trial in the NICU. Clin Neurophysiol. 125:675–684.

Wendel K, Vaisanen O, Malmivuo J, Gencer NG, Vanrumste B, Durka P, Magjarevic R, Supek S, Pascu ML, Fontenelle H, Grave de Peralta MR. 2009. EEG/MEG source imaging: methods, challenges, and open issues. Comput Intell Neurosci.656092.

Witte H, Putsche P, Eiselt M, Schwab K, Wacker M, Leistritz L. 2011. Time-variant analysis of phase couplings and amplitude-frequency dependencies of and between frequency components of EEG burst patterns in full-term newborns. Clin Neurophysiol. 122:253–266.

Wolpaw JR, Wood CC. 1982. Scalp distribution of human auditory evoked potentials. I. Evaluation of reference electrode sites. Electroencephalogr Clin Neurophysiol. 54:15–24.

Wolters CH, Kuhn M, Anwander A, Reitzinger S. 2002. A parallel algebraic multigrid solver for finite element method based source localization in the human brain. Comp Vis Sci. 5:165–177.

Womelsdorf T, Schoffelen JM, Oostenveld R, Singer W, Desimone R, Engel AK, Fries P. 2007. Modulation of neuronal interactions through neuronal synchronization. Science. 316:1609–1612.

Yakovlev PI, Lecours AR. 1967. The myelogenetic cycles of regional maturation of the brain. In: Minkowski A, editor. Regional development of the brain in early life. Blackwell Science, Oxford. p 3–70.

Yamazaki M, Tucker DM, Terrill M, Fujimoto A, Yamamoto T. 2013. Dense array EEG source estimation in neocortical epilepsy. Front Neurol. 4:42.

Yan Y, Nunez PL, Hart RT. 1991. Finite-element model of the human head: scalp potentials due to dipole sources. Med Biol Eng Comput. 29:475–481.

Yang JW, Hanganu-Opatz IL, Sun JJ, Luhmann HJ. 2009. Three patterns of oscillatory activity differentially synchronize developing neocortical networks in vivo. J Neurosci. 29:9011–9025.

Yao D, Wang L, Arendt-Nielsen L, Chen AC. 2007. The effect of reference choices on the spatio-temporal analysis of brain evoked potentials: the use of infinite reference. Comput Biol Med. 37:1529–1538.

Yao D, Wang L, Oostenveld R, Nielsen KD, Arendt-Nielsen L, Chen AC. 2005. A comparative study of different references for EEG spectral mapping: the issue of the neutral reference and the use of the infinity reference. Physiol Meas. 26:173–184.